Calhoun: The NPS Institutional Archive

DSpace Repository

Theses and Dissertations 1. Thesis and Dissertation Collection, all items

1969

A computer study of channeling in silicon

Finno, Roy Stephen

Monterey, California. Naval Postgraduate School

http://hdl.handle.net/10945/24643

This publication is a work of the U.S. Government as defined in Title 17, United States Code, Section 101. Copyright protection is not available for this work in the United States.

Downloaded from NPS Archive: Calhoun

Calhoun is the Naval Postgraduate School's public access digital repository for research materials and institutional publications created by the NPS community. Calhoun is named for Professor of Mathematics Guy K. Calhoun, NPS's first appointed -- and published -- scholarly author.

Dudley Knox Library / Naval Postgraduate School
411 Dyer Road / 1 University Circle
Monterey, California USA 93943

http://www.nps.edu/library

NPS ARCHIVE
1969
FINNO, R.

A COMPUTER STUDY OF CHANNELING IN SILICON

by

Roy Stephen Finno

DUDLEY KNOX LIBRARY
NAVAL POSTGRADUATE SCHOOL
MONTEREY, CA 93943-5101

United States Naval Postgraduate School

THESIS

A COMPUTER STUDY OF CHANNELING IN SILICON

by

Roy Stephen Finno

June 1969

This document has been approved for public release and sale; its distribution is unlimited.

1133284

LIB
NA TE SCHOOL
MONTEREY, CALIF. 93940

A Computer Study of Channeling in Silicon

by

Roy Stephen Finno
Captain, United States Army
B.S., United States Military Academy, 1964

Submitted in partial fulfillment of the
requirements for the degree of

MASTER OF SCIENCE IN PHYSICS

from the

NAVAL POSTGRADUATE SCHOOL
June 1969

NPS ARCHIVE
1969
FINNO, R.

~~Thesis
F465
c.1~~

ABSTRACT

A computer simulation study of channeling in a diamond lattice. The simulation was done for a xenon ion striking the (100), (110) or (111) surface of a silicon target. Potential functions for the Si-Si lattice bond and the Xe-Si interaction are postulated. The electronic stopping cross section for the $\langle 110 \rangle$ channel of silicon is estimated.

This work is a continuation in the development of a computer model formulated at the USNPGS which takes into consideration the displacement of the atoms in the target lattice as well as inelastic energy losses by the primary ion. The lattice was not thermalized and only the repulsive portion of the lattice-lattice potential was utilized. Computed ranges are in good agreement with experimental date.

LIBRARY
NAVAL POSTGRADUATE SCHOOL
MONTEREY, CALIF. 93940

DUDLEY KNOX LIBRARY
NAVAL POSTGRADUATE SCHOOL
MONTEREY, CA 93943-5101

TABLE OF CONTENTS

I. INTRODUCTION---------- 9

II. STUDY OBJECTIVES---------- 11

III. SIMULATION MODEL---------- 12

IV. PROCEDURE---------- 14

V. POTENTIAL FUNCTION AND INELASTIC LOSS CONSTANT----- 15

A. Si-Si BOND---------- 15

B. INELASTIC LOSS CONSTANT---------- 17

C. Xe-Si POTENTIAL---------- 19

VI. RESULTS---------- 22

A. ⟨100⟩ CHANNEL---------- 22

B. ⟨110⟩ CHANNEL---------- 23

C. ⟨111⟩ CHANNEL---------- 25

VII. CONCLUSIONS---------- 28

APPENDIX A - LATTICE GENERATOR---------- 30

APPENDIX B - CALCULATION OF FORCES AND POTENTIALS-------- 36

APPENDIX C - PROGRAM PARAMETERS---------- 41

COMPUTER PROGRAM - SUBROUTINE DL100---------- 43

COMPUTER PROGRAM - SUBROUTINE DL110---------- 45

COMPUTER PROGRAM - SUBROUTINE DL111---------- 47

COMPUTER PROGRAM - EXPONENTIAL INTERPOLATOR---------- 49

LIST OF REFERENCES---------- 77

INITIAL DISTRIBUTION LIST---------- 79

FORM DD 1473---------- 81

LIST OF FIGURES

Figure

1. The (100) surface of silicon with the ⟨100⟩ channel indicated.

2. The (110) surface of silicon with the ⟨110⟩ channel indicated.

3. The (111) surface of silicon with the three similar ⟨111⟩ channels indicated.

4. The shape and relative sizes of the three major channels in silicon.

5. Range distribution curves for 40 KeV ^{125}Xe in silicon.

6. Radial Electron Density functions for a number of Si ions are compared.

7. IPF's for various identical ion interactions of Si are shown. The Gibson II function is included for comparison.

8. Radial Electron Density functions for the neutral and +6 ionic states of xenon.

9. IPF's for the Xe^{+6}-Si^{+1} and Xe^{+6}-Si^{+4} interaction. Two Born-Mayer approximations are shown.

10. A composite potential function for the Xe^{+6}-Si^{+4} interaction.

11. dE/dx vs ion energy for a well channeled Xe^{125} ion in the ⟨100⟩ channel of silicon.

12. dE/dx vs $E^{\frac{1}{2}}$ for a well channeled Xe^{125} ion in the ⟨100⟩ channel of silicon.

13. Range Profile for a 5 KeV Xe^{125} ion in the ⟨100⟩ channel of silicon.

14. Range Profile Section for a 5 KeV Xe^{125} ion in the ⟨100⟩ channel of silicon.

15. Deviation of a well channeled 5 KeV Xe^{125} ion from the center of the ⟨100⟩ channel of silicon.

16. Range Profile Section for a 5 KeV Silicon ion in the ⟨100⟩ channel of silicon.

17. dE/dx vs ion energy for a well channeled Xe^{125} ion in the ⟨110⟩ channel of silicon for various values of CELS.

18. dE/dx vs $E^{\frac{1}{2}}$ for a well channeled Xe^{125} ion in the ⟨110⟩ channel of silicon.

$$CELS = -\ 8 \times 10^{14}\ \frac{n\text{-}sec}{m^2}$$

19. Range Profile of a 5 KeV Xe^{125} ion in the ⟨110⟩ channel of silicon.

20. Range Profile Section for a 5 KeV Xe^{125} ion in the ⟨110⟩ channel of silicon.

21. Ranges at various impact points for Xe^{125} ions in the ⟨110⟩ channel of silicon.

22. The ⟨111⟩ channel of silicon with the channel centers indicated.

23. dE/dx vs ion energy for a well channeled Xe^{125} ion in the ⟨111⟩ channel of silicon.

24. dE/dx vs $E^{\frac{1}{2}}$ for well channeled Xe^{125} ions in the ⟨111⟩ channel of silicon.

25. dx/dE vs ion energy for a well channeled Xe^{125} ion in the ⟨111⟩ channel of silicon compared to an actual 20 KeV run in the ⟨111⟩ channel of silicon.

26. Range of a 5 KeV Xe^{125} ion at the various impact points in the ⟨111⟩ channel of silicon.

ACKNOWLEDGEMENT

A digital computer simulation requires the cooperation of many personnel not directly concerned with the project. I am indebted to the operators on the second and third shifts at the computer facility fortheir assistance in insuring rapid turn around time on my programs. I would like to extend thanks to LCDR Walter Moore for the many hours he spent helping me to understand the basic simulation model for channeling.

I am especially grateful to Dr. Don E. Harrison, Jr., of the Naval Postgraduate School for his supervision and assistance during this project. To my wife, Judith, I express my appreciation for her patience, understanding and assistance in preparation of his manuscript.

I. INTRODUCTION

Experimental and theoretical studies over the past decade have established that the slowing down of ions in crystals is strongly dependent on the crystallographic orientation of the lattice with respect to the direction of the incident beam. [1,2,3,4,5] This effect is known as channeling. A particle moving along one of the major axis of a crystal may be "steered" (i.e. its momentum redirected toward the center of the channel) by successive gentle collisions with the "strings" of atoms that comprise the "walls" of the channel. Davies et al [1] reported that this channeling effect increases the mean range of Xe^{125} by as much as a factor of 10 over the values observed in a non-crystalline solid of similar atomic number.

Earlier computer studies performed at the NPGS investigated channeling in the body centered [6] and face centered cubic lattice. [7] This thesis is an extension of this previous work into the diamond lattice.

When a substrate is bombarded by a beam of incident energetic particles it will lose some of its own ions by sputtering and retain some of the incident ions. The incident ions retained are said to be implanted, and the technique of using an energetic ion beam to introduce ions into a substrate is called ion implantation. [5] This doping technique in silicon should be very effective due to the extremely open nature of its lattice and its large channel sizes.

The difference in the depth of penetration of energetic particles along the principal channels in silicon may be attributed to the various channel sizes. Figures 1-3 show the locations of the various channels in the (100), (110) and (111) surfaces of silicon while Fig. 4 is a "ball and stick" model showing the relative shape and sizes of the three principal channels in silicon. According to Davies [1] and Manchester [8] the preferential order of channeling would occur along the ⟨110⟩, ⟨111⟩ and ⟨100⟩ channels in decreasing order with the ⟨111⟩ channel only marginally better than the ⟨100⟩ channel. This fact is graphically indicated in Fig. 5.

Much work over the past several years has been devoted to studying this channeling effect in silicon. Manchester [8] has studied the feasibility of forming metallurgical junctions in silicon by making use of the channeling phenomenon. Eisen [9] has studied the channeling of medium mass ions through silicon with special attention directed toward the electronic stopping cross section of well channeled ions. Davies and his co-workers have written a series of papers [2,3,4,10] discussing the penetration of KeV and MeV projectiles in silicon and the disordering of the lattice caused by this ion bombardment. Glotin [11], Nelson and Mazey [12], and Dearnaley et al [13] have investigated the implantation of phosphorous in silicon. Eriksson et al [14] have studied the implantation and annealing behavior of Group III and V ions in silicon. Gibbons [5] sums up the current theoretical and experimental work pertinent to the problem of predicting impurity distribution profiles in implanted material.

II. STUDY OBJECTIVES

This report is an extension of the NPGS channeling model from the bcc and fcc orientations into the diamond lattice. This thesis attempts to establish, with xenon as the bullet and silicon as the target, the following characteristics for the three major channeling orientations:

a) The potential between the bullet and the lattice,

b) A value for the electronic stopping power, and

c) The ion implantation profile at 5 KeV.

III. SIMULATION MODEL

The basic model has been developed by the NPGS group over the past six years. A brief description of this model and the alterations made for this study follow but for detailed presentations the reader is referred to Refs.7,15 and 16.

The simulation model consists of a single primary and a silicon (diamond) lattice target containing between 60 and 150 atoms. All runs were made with the primary (bullet) striking the target normally, although the program is sufficiently flexible that the bullet could be fired into the target at any angle.

The silicon target lattice as used in this simulation is composed of a central core and a surrounding shell. The program is structured so that the bullet is never allowed to leave this central core. In addition, in the (110) and (111) orientations the shell atoms were not permitted to move. This allows the program to run slightly faster and also tends to hold the core atoms in place for a slightly longer time. The shell atoms were not allowed to displace in the (100) channeling direction. Even with the shell atoms displacing, given a bullet energy and an equivalent channeling location in the (111) and (100) orientations, the (100) channeling program ran faster. For a detailed discussion of the lattice generator to include the dividing of the target crystal into active core and passive shell see Appendix A.

In previous computer simulations the interatomic potential function and force function were of the exponential (Born-Mayer) type

$$F = \exp(A + Bx)$$

where A and B are empirically determined constants and x is the atomic separation. The functions are not always of this type in this simulation, and force and potential tables were constructed. For details of this scheme see Appendix B.

Two major assumptions are made in this simulation model,

(1) The bullet moves in a perfect lattice undisturbed by the thermal displacements of the atoms.

(2) Only repulsive forces between the lattice atoms have been included.

While both of these assumptions are obviously erroneous, previous studies have shown that this simulation model is still a good first order approximation for channeling.

IV. PROCEDURE

This simulation study was conducted in an IBM 360/67 computer using FORTRAN IV language.

The computer sets up the diamond lattice in the desired orientation (see Figs. 1-4) and starts a xenon ion into it. A brief study of the symmetry of the target lattice shows that the indicated impact areas cover all the possible points for the three orientations of silicon. Within these impact areas, several points, depending on the orientation of the lattice, were selected as representative of the channel. In the determination of how many points were to be chosen in each impact area, consideration was given to obvious lattice symmetry and to computer running time.

Various combinations of Bullet-Target Potentials and CELS, a constant used to determine inelastic energy losses, were tried at different bullet energies and the maximum range of the bullet for each orientation was matched against experimental range data as reported by Davies et al [1].

Channel profiles for 5 KeV xenon atoms were determined for the (100), (110), and (111) channels of silicon. Runs were made to determine dE/dx for each major axis in silicon and maximum ranges for xenon at higher energies were determined knowing

$$R = \int_0^E \left(\frac{dE}{dx}\right)^{-1} dE \ .$$

V. POTENTIAL FUNCTIONS AND INELASTIC LOSS CONSTANT

The purpose of this section is to discuss first, the determination of the potentials used to approximate the Si-Si lattice bond and the xenon-silicon bullet-lattice interaction, and second, the determination of an inelastic loss constant. Presently, there exists in the literature calculated potentials for the Si-Si system [17] but none for the Xe-Si system. Eisen [9] has published experimental electronic stopping cross sections for medium mass ions in silicon but no data exists for xenon in silicon.

A. Si-Si BOND

The starting point for selecting a potential for the Si-Si bond are the Interaction Potential Functions (IPF) as calculated by Harrison [17]. These potentials are only the repulsive portion of the potential function for pairs of particles and neglect any lattice effects. Harrison [17] also indicates that they are most likely too "hard". Figure 6 shows the radial electron density for Si. Since this radial electron density was determined using a spherical approximation, it is not correct for $r \geq 1.5a_H$ (a_H = Bohr Radius = 0.529Å) [17]. Figure 7 shows several different potential functions for the Si-Si bond with the Gibson II for comparison. The Si-Si and Si-Si$^+$ IPF's show approximately the correct behavior and zero close to the nearest neighbor distance for silicon. The Si^{+1}-Si^{+1} also shows approximately the correct behavior but fails to zero at the nearest neighbor distance. Curve 3 of Fig. 7 is the Si^{+1}-Si^{+1} IPF forced to zero at the nearest neighbor distance.

Any one of these three potentials (Si-Si, Si-Si^{+} or Si-Si^{+} (zeroed)) will serve as a good approximation for the Si-Si bond. It is obvious that the Gibson II will not serve as a good representation of this bond.

The covalent bonding between Silicon atoms has the effect of concentrating about 0.5 of an electron of the outer shell along every chemical bond [18]. Therefore, it seems reasonable to conclude that each silicon atom along the Si-Si bond sees the other in a slightly ionized state but not completely ionized to the +1 state due to the shielding effects of this shared electron. This would seem to eliminate the Si-Si and Si^{+1}-Si^{+1} potentials for the Si-Si bond and lead to the selection of the Si-Si^{+} potential as representing the bond. It was noted earlier, however, that the IPF's are probably too hard. Therefore, the Si^{+1}-Si^{+1} (zeroed) potential was chosen as representative of the bond potential as it is "softer" than the Si-Si^{+} potential and is forced to zero at the nearest neighbor distance.

Admittedly the reasons for choosing the Si^{+}-Si^{+} potential were rather arbitrary but the reader is asked to keep three points in mind. First, all three potentials are approximately equal and trial runs indicated no significant effect on the range when these potentials were interchanged. Second, the neutral silicon atoms are too large to fit into the Si lattice. Third, the two overwhelming factors that control channeling ranges are the bullet-lattice potential and the inelastic loss approximation. Any reasonably potential selected for the Si-Si bond should have no discernable effect on these ranges.

B. INELASTIC LOSS CONSTANT

One of the principal mechanisms of energy loss for channeled ions in a solid is the interaction of the ion with electrons (both bound and free) of the solid. This computer study accounts for this loss through the use of a "frictional force multiplier" which acts on the ions velocity in a manner to produce a "drag" force on the incident ion. This "friction force multiplier" is directly proportional to the electronic stopping cross section.

Eisen [9] reports electronic stopping cross sections (S_e) for medium mass ions ($5 \leq Z \leq 19$) in the $\langle 100 \rangle$, $\langle 110 \rangle$, and $\langle 111 \rangle$ channels of silicon. In unpublished data [19] he extends S_e for the $\langle 110 \rangle$ channel by allowing the atomic number of the incident ion to increase up to $Z = 36$ (Krypton). Eisen's data reveals the following: first, S_e was found to exhibit a strong oscillatory dependence on Z, the atomic number of the incident ion, second, S_e is lowest in the $\langle 110 \rangle$ channel and third, S_e is approximately equal in the $\langle 111 \rangle$ and $\langle 100 \rangle$ channels.

No data presently exists in the literature for the electronic stopping cross section of xenon in silicon. However, based on previous computer studies of channeling in copper and tungsten undertaken at NPGS the frictional force multiplier was estimated to be 1.0×10^{-13} n-sec/m in the $\langle 100 \rangle$ channel. Using Eisen's data [19] and noting the ratio between S_e in the $\langle 100 \rangle$ and $\langle 110 \rangle$ channels, the frictional force multiplier in the $\langle 110 \rangle$ channel is approximately -8×10^{-14} n-sec/m. These values were used in this computer study.

Ericksson et al [20] give estimates of electronic stopping cross section for various ions along the $\langle 100 \rangle$ and $\langle 110 \rangle$ channels of tungsten. Their data also indicates that S_e shows a strong oscillatory dependence on Z, the atomic number of the incident ion and this oscillatory dependence is very similar to the dependence Eisen [9,19] found for ions channeled in silicon. If the assumption is made that the ratio between stopping cross sections for xenon and krypton (which is chemically similar to xenon) channeled in tungsten is approximately the same as the ratio between these ions channeled in silicon, one obtains a value of

$$8.5 \times 10^{-14} \frac{\text{eV-cm}^2}{\text{atom}} \quad (\text{where } v = 1.0 \times 10^8 \text{ cm/sec})$$

as an estimate of S_e in the $\langle 110 \rangle$ channel in silicon. This converts to a value of 7×10^{-14} n-sec/m as a frictional force multiplier for the $\langle 110 \rangle$ channel and is in good agreement with the value used in this computer study.

$$\text{CELS} = \frac{S_e(v) \cdot \eta \cdot 1.6 \times 10^{-19} (\text{J/eV})}{v(\text{cm/sec}) \times 10^{-4} (\text{m}^2/\text{cm}^2)} \quad \text{where } \eta = \text{number density.}$$

The author does not make any claim that the values of the "frictional force" used in this study are "correct". It is felt, however, that based on a study of Eisen's data [9,19] and the extrapolation described above, the values chosen for S_e will certainly be within 20% of the experimentally determined values and more than likely will be much closer than that.

C. Xe-Si POTENTIAL

As in the case of the Si-Si bond, no potential function exists for the xenon-silicon interaction. Therefore, the Interaction Potential Functions will again serve as a starting point for selecting the Xe-Si potential. Figure 8 shows the radial electron density for xenon in the nonionized and +6 ionization state, while Fig. 9 shows the IPF for Xe^{+6}-Si^{+4} and Xe^{+6}-Si^{+1}.

Far from the Si-Si bond, the electron density for silicon should approach the Si^{+4} distribution (Fig. 6). Special note should be taken of the ⟨111⟩ channel of silicon where the atoms bounding the channel have one of their bonds parallel to the centerline of the channel. Determing the ionization state of xenon is also difficult. Harrison [17] has found for Xe-W system a good potential fit can be found if xenon is assumed to be in the +6 or +8 ionization state, even though this high ionic state is somewhat surprising. The Xe^{+}-W^{+6} potential was found to be unrealistically strong. As a result, of the above it was concluded that the Xe^{+6}-Si^{+4} IPF was a good starting point for the bullet-lattice potential.

The Xe^{+6}-Si^{+4} IPF (Fig. 9) diverges to unrealistically strong values at large separations. This divergence is characteristic of the theoretical model used to calculate the IPF and is not characteristic of the physical system [17]. A Born-Mayer approximation for the Xe-Si interaction would fail at small separations because it would approach a finite value at zero separation, while the actual Xe-Si function should approach a pure coulomb potential at small separations. Our final choice of the potential to represent the Xe-Si system incorporated both of the above approximations. For separations less than $1.2a_H$ the IPF was used, while a Born-Mayer approximation was constructed for separations greater than $1.2a_H$.

Curve BM1 (Fig. 9) when used in conjunction with the previously discussed values of the "frictional force" parameter gives excellent results for xenon ions injected in the ⟨110⟩ and ⟨100⟩ channels, however, it is a poor approximation for xenon in the ⟨111⟩ channel. After several trial runs it became obvious that all three channeling directions could not fit on one Born-Mayer approximation. The maximum range in the ⟨111⟩ channel could be forced to approach the experimental range if the "frictional force" constant is decreased by two orders of magnitude. This is unrealistic since it conflicts drastically with Eisen's [9] experimental data.

A solution to the problem was to make a separate Born-Mayer approximation for the ⟨111⟩ channel; this is curve BM2 in Fig. 9. Intuitively, one feels that this answer is not the correct one. All previous studies have found that one potential satisfies all channeling directions. However, two points should be kept in mind. First, all previous computer studies dealt with channeling in a metallic target where the principal method of bonding between lattice atoms is metallic. This is the first computer study where the bonding between the lattice atoms is co-valent and any conclusions drawn for a metallic target need not necessarily be true in silicon. Secondly, the orientation of the bond between silicon atoms with relation to the channeling directions varies among all three principal channels of silicon. As previously mentioned, the extreme is reached in the ⟨111⟩ channel where the Si-Si bond is parallel to the center line of the channel. This more than likely has an effect on the silicon charge distribution as seen by the xenon ion and could possibly cause the potential for the ⟨111⟩ channel to differ from the other channels.

Another possibility is that a Born-Mayer approximation is not valid in silicon. A picture of the Xe^{+6}-Si^{+4} potential might be obtained by combining the portion of the three curves: IPF, BM1 and BM2 that we know give us accurate results. Such a composite curve is shown in Fig. 10. It is obvious that this composite curve is unrealistic.

VI. RESULTS

A. ⟨100⟩ CHANNEL

Figure 11 is a plot of dE/dx(in ^{eV}/LU) versus ion energy for a perfectly channeled xenon ion in the ⟨100⟩ direction. (Note 1LU = 2.71Å = 0.0646 $\mu g/cm^2$). Between 30-100 KeV, dE/dx is approximately proportional to the energy indicating that in this region the elastic and inelastic collision processes are both exerting a significant influence. This agrees with experimental data reported by Davies [1].

Figure 12 is a plot of dE/dx versus $E^{\frac{1}{2}}$. Above 800 KeV dE/dx is proportional to $E^{\frac{1}{2}}$ indicating that as expected the inelastic process is the primary loss mechanism. Both Figs. 11 and 12 show that below 20 KeV the elastic collision process is primarily responsible for slowing down the ion.

Figures 13 and 14 are range profiles and range profile sections for the ⟨100⟩ channel. Figure 13 shows only one-half of the channel, the range profile for the other half is very similar but not identical to this.

Table 1 (below) is a comparison between experimental ranges obtained by Davies [1] and computer calculated ranges for the ⟨100⟩ channel. The column labeled dE/dx is the range value obtained by using the dE/dx curve in Fig. 11 and the relationship

$$R = \int_0^E (dE/dx)^{-1} \, dE \; .$$

The computer calculated range at 40 KeV, although higher than the experimental value reported by Davies, falls within his ±3% error estimate.

Range ⟨100⟩

Energy	Experimental	dE/dx	Computer
5	--	60	69.7
20	491.7*	485	490.2
40	1162.7	1230	1193.8

Table I. Energy in KeV, range in LU

*Experimental range for 20 KeV extrapolated from Davies [4] experimental data.

In a bcc or fcc crystal an ion injected into the center of the channel remains there. This is not the case for an ion injected into the center of the ⟨100⟩ channel of silicon. The ion "wobbles" slightly around the channel center oscillating between (110) planes. (Fig. 15) Note the similarity of the orbit in the second and fourth quadrant.

Figure 6 is a Range Profile Section for a 5 KeV silicon ion injected into the ⟨100⟩ channel of silicon. Although no experimental data exists to compare maximum ranges it is interesting to note that the range profile section is very similar to the range profile of xenon in silicon.

B. ⟨110⟩ CHANNEL

Figure 7 is a plot of dE/dx versus energy at various values of CELS (analogous to electronic stopping power) for a xenon ion injected into the center of the ⟨110⟩ channel. It is apparent that the energy loss is very sensitive to CELS especially at higher energies indicating that electronic stopping is the principle mechanism of energy loss for well channeled ions in the ⟨110⟩ direction. Figure 18 is a plot of dE/dx versus (ion energy)$^{\frac{1}{2}}$ for well channeled ions with CELS = - 8 x 10^{-14} n-sec/m, the value selected for use in this study. dE/dx is proportional to $E^{\frac{1}{2}}$ at incident ion energies greater than 2 KeV again indicating that electronic stopping is the principle loss mechanism.

Figure 19 and Fig. 20 are a range profile and a range profile section for the ⟨110⟩ channel. Both show only half the channel although the other half of the channel should be identical. While it is apparent that the ⟨110⟩ channel is a preferred channeling direction the maximum range falls off rapidly if the ion is injected slightly off center. (For example, if the ion is injected approximately 0.2LU from the center of the channel the maximum range decreased by one-half). Of particular interest is point 1 in the Range Profile Section (Fig. 20). An ion injected at this point in the channel has a range of 100LU which is much greater than expected. The xenon ion injected here is strongly influenced by the silicon atom located at position C which forces it into the center of the channel and adds significantly to its range.

Table II is again a comparison between ranges obtained experimentally by Davies [1] and computer calculated ranges.

Range 110

Energy	Experimental	dE/dx	Computer
5	--	1090	1094
20	2371	2400	--
40	3812	3800	--

Table II. Ranges in LU, Energies in KeV.

The ranges calculated using dE/dx are in good agreement with experimental ranges obtained by Davies [1]. No attempt was made to channel a 20 KeV xenon ion as it would be too expensive in computer running time (approximately 90 minutes).

Figure 21 shows, the ranges obtained for selected points in the ⟨110⟩ channel when the energy of the incident xenon ion was increased to 20 KeV. Two points should be noted. First, the channel "expands" at higher energy as expected. Second, a comparison of the range of the ion incident on point 1 with the range obtained when the incident ion energy was 5 KeV (Fig. 20) shows that the large range for the 5 KeV ion is a low energy phenomenon.

C. ⟨111⟩ CHANNEL

Figure 22 is an enlargement of the ⟨111⟩ channel. Initially, point 1 was thought to be the center of the channel but subsequent probing of the channel proved this assumption to be incorrect. The points numbered 2 and 3 are actually the channel "centers". If atoms A, B, D and B, C, D are thought to form triangles, as indicated, then points 2 and 3 may be considered the center of their respective triangle equidistant from the atoms that form the triangle's vertices. Additionally, although the basic shape of the channel remains unchanged, the atoms that bound the channel do not necessarily lie in the planes indicated in Fig. 22. Two other possible configurations are: (a) atoms A and C in the front plane, B in the third plane and D in the fifth plane or (b) atoms A and C in the fifth plane back, D in the third plane back and B in the front plane. These three channel configurations are shown in Fig. 3. They affect the ion only as it initially enters the lattice, by determining in which direction it will be initially steered and have almost no effect ($\leq 0.5\%$) on the calculated maximum range.

Figure 23 and 24 are plots of dE/dx vs ion energy, E and $E^{\frac{1}{2}}$. Up to 100 KeV both elastic and inelastic collisions are both important loss mechanisms. Below 20 KeV, elastic losses appear to predominate.

Figure 25 shows dx/dE curves for xenon in the $\langle 111 \rangle$ channel. The area under these curves should be an accurate representation of the total range travelled by an incident xenon ion. The solid curve (I) was obtained by injecting xenon ions into the center of the $\langle 111 \rangle$ channel at various energies, allowing them to penetrate the lattice for a short distance ($\leq$ 5LU) and determining the energy loss of the xenon ion per lattice unit. The dotted curve (II) is actually a 20 KeV run for a xenon ion initially injected in the center of the $\langle 111 \rangle$ channel and followed until it finally stops in the crystal. The difference between these two curves can be accounted for by noting that an ion injected into the center of the ⟨111⟩ channel deviates considerably from the channel center (up to .09LU) as it passes thru the crystal and that this deviation increases as the ion energy decreases. Therefore, the implicit assumption made in determining curve I, that the ion remains in the center of the ⟨111⟩ channel as it passes through the crystal is incorrect and will introduce large errors (up to 20%) in ranges at the low end of the energy spectrum where the elastic loss mechanism predominates. Table III is a summary of maximum ranges obtained at various energies for the ⟨111⟩ channel.

Range ⟨111⟩

Energy	Experimental	Curve I	Curve II	Computer
5	--	37	60	57
20	511	417	500	511
40	1209	1050	1170	--

Table III. Energy in KeV, range in LU.

Figure 26 is a representation of the ⟨111⟩ channel and shows ranges obtained at different initial impact points in the channel. Two things can be noted about the range distribution. First, there is a definite peak at the center of the channel and secondly, the total range is extremely dependent on exact impact point in the channel. This last fact makes it impossible to draw any meaningful range profiles or ranges profile section.

VII. CONCLUSIONS

1. Maximum channeled ranges were fit to experimental data at 20 KeV.

2. For the ⟨100⟩ and ⟨111⟩ channels both elastic and inelastic losses are important between 20 and 80 KeV.

3. Inelastic losses become predominant at energies greater than 400 KeV for the ⟨100⟩ channel.

4. Inelastic loss seems to be the predominant loss mechanism for well channeled ions in the ⟨110⟩ channel even at low energies (~2 KeV).

5. The range in the ⟨111⟩ channel is extremely sensitive to impact parameter and appears to possess no symmetry.

6. S_e was determined to be $8.5 \times 10^{-14} \frac{\text{eV-cm}^2}{\text{atom}}$ in the ⟨110⟩ channel of silicon. In the ⟨100⟩ and ⟨111⟩ channels $S_e = 10.6 \times 10^{-14} \frac{\text{eV-cm}^2}{\text{atom}}$ ($v = 1.0 \times 10^8$ cm/sec).

7. All three channeling directions for xenon in silicon can not be determined using the same Born-Mayer Potential Function. A minimum of two Born-Mayer Potentials are required.

8. At low energies the ⟨100⟩ channel is the preferential direction for channeling when compared to the ⟨111⟩ channel. This is the reverse of the situation for incident ions energies greater than 20 KeV.

9. Although the potentials and the "frictional force" constant were discussed separately it can not be overemphasized that all three of these variables must be treated as an integrated whole. A change in either the bullet-target potential or the frictional force constant has a profound effect on the maximum channeled range especially in the ⟨110⟩ orientations. The final selection of the Born-Mayer approximations to the Xe-Si interactions, the frictional force parameter and Si-Si bond potential seems to represent the best of all the parameters.

APPENDIX A (LATTICE GENERATOR)

Previous computer studies undertaken by the NPGS Group over the past several years have dealt exclusively with the body centered and face centered cubic lattices. In building the diamond lattice, which is basically two interpenetrating face centered cubic lattices, the primary aim was to construct the lattice in such a way that only mimimum modifications on the basic computer model for channeling would be necessary. The diamond lattice generator was constructed so that no major change in the basic lattice regenerator was necessary. Therefore, to understand the lattice generator, it is necessary to understand the fundamental mechanism behind the regenerator subroutine.

Subroutine REGEN works as follows:

(1) It receives the parameter MSS from the main program which indicates the direction of regeneration (±X, ±Y, ±Z).

(2) It checks every atom in the crystal against a constant which depends on the direction of regeneration and either

a. discards the atom since the bullet has passed and is no longer under its influence, or

b. shifts and renumbers the atom while preserving its velocity components.

(3) It builds and undisturbed section crystal in the direction of travel of the bullet.

(4) It shifts the bullet to its proper location in the rebuilt crystal preserving its velocity components.

Schematically, this is done as follows: (The crystal regenerates when the bullet passes plane E)

A) Crystal Prior to Regeneration

Direction of Travel

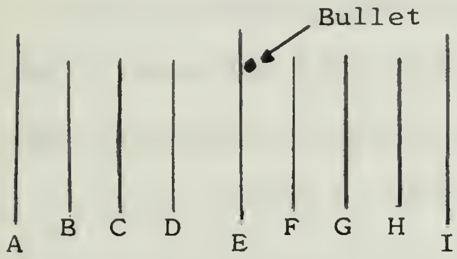

The follwing planes are identical:
A - E - I
B - F
C - G
D - H

Disordered Crystal,
Passed By Bullet

B) Crystal During Regeneration

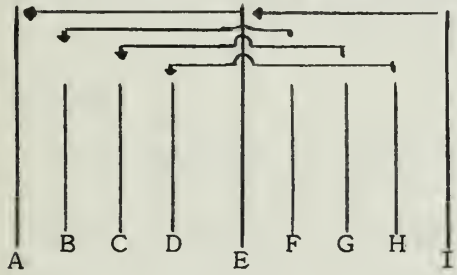

Plane E goes to A
F " " B
G " " C
H " " D
I " " E
Old planes A,B,C,D,
discarded

Discarded

C) Crystal After Regeneration

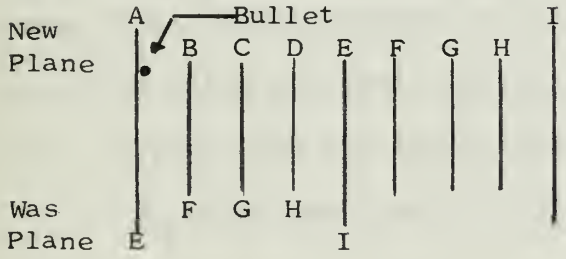

Planes F,G,H,I are newly constructed as part of a perfect crystal lattice.

This scheme discards the portion of the crystal the bullet has passed through and builds an undisturbed portion of the crystal in front of the bullet.

To build a crystal which will fit into the regeneration scheme the crystal generator must:

(1) Construct one plane at a time in the Y direction. It places the first atom in the Y = 0 plane at the lowest value of X and Z (0,0) and continues placing atoms at increasing values of X for fixed Z, then increases the value of Z and repeats the process until the plane is completed. The next Y plane is constructed in a similar manner and additional Y planes are constructed until the microcrystallite is completed. It assigns a number to each atom. A completed Y = 0 plane for the (100) orientation has atoms positioned and numbered as follows

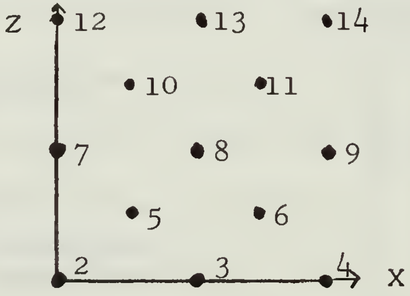

Planes must be generated in this manner.

(2) Build the following symmetry into the crystal. The left and right face are identical to each other and identical to one plane in between them. There is similar symmetry between the front and back faces as well as the bottom and top faces.

This symmetry in the lattice allows the regenerator to operate as follows:

(1) It checks the location of each atom in the crystal to see if it is to be regenerated (shifted).

(2) If it is to be regenerated, a fixed number (IDX, IDY, or IDZ depending on the direction of regeneration) is subtracted from the atom number. This partially shifts the atom into its identical plane.

(3) The regenerator then subtracts (or adds) DXT, DYT, or DZT from one of theatom's co-ordinates depending on the direction of regeneration. This completes the movement of the atom into its identical plane.

(4) As previously mentioned the regenerator preserves the velocity components and potential energies of all atoms regenerated.

(5) The bullet is regenerated in a similar (but not identical) manner.

In addition to being tailored to fit SUBROUTINE REGEN the lattice generator, through the use of a variable LCUT, breaks the lattice into an active core and a surrounding shell. This is an absolute necessity due to the large size of the crystal which was dictated by the symmetry requirements of SUBROUTINE REGEN. (Orientation (100) contains 96 atoms, orientation (110) contains 60 atoms and orientation (111) contains 146 atoms). LCUT does this in the following way:

1) Any atom in the active portion of the crystal is given an LCUT = 0. This allows it to interact with any other atom in the crystal.

2) Any atom in shell is given an LCUT = 1 which allows it to interact only with core atoms and not with any shell atoms.

The lattice generator subroutine also contains the constants XLL, XLF, ZLL, ZLF which are used to determine when the lattice is to be regenerated. They are chosen to insure that the bullet always remains in the core and the lattice regenerates when the bullet is about to leave the core and enter the shell.

As an example, a 20 KeV Xe^{125} atom in the center of the ⟨100⟩ channel of silicon has a range of 491.7 LU and the program runs for 35 minutes and 39 secs. With the LCUT package inserted into the program the calculated range is 490.2 LU with a program running time of 13 minutes and 12 seconds. The LCUT package is obviously effective for it conserves computer time without sacrificing any accuracy in range calculations.

In summary, the Lattice Generator

(1) Contains all the constants necessary to regenerate the lattice,

(2) It constructed, with appropriate tests, to insure that it fits into the scheme necessary for Subroutine REGEN, and

(3) Contains the LCUT package which reduces the number of active atoms in the crystal, thus conserving running time.

An alternative to building the lattice generator to fit subroutine REGEN would be to construct a smaller active crystal, eliminate the LCUT package and rewrite the REGEN subroutine to fit the lattice generator. This method was not chosen for the following reasons:

(1) It was easier to modify the existing lattice generator to fit the old Subroutine REGEN than to start from scratch and build a new Regeneration Subroutine and Lattice Generator Subroutine tailored for each other, and

(2) Simple modifications in the generator alone would not drastically alter the existing Channeling Program which had proved to be an accurate representation of the channeling process in fcc and bcc crystals.

APPENDIX B (CALCULATION OF FORCES AND POTENTIALS)

A major change in procedure was introduced in the calculation forces and potentials. In previous models the interatomic potential function and force functions were of the exponential type,

$$F = \exp (A + Bx)$$

where A and B were empirically determined constants and x is the atomic separation. The atomic separation was determined, substituted into the appropriate function and the force and potential determined.

This computer simulation determined forces and potentials as follows. First, a set of potentials (in Rydbergs) derived from Interaction Potential Functions are read into the program for the lattice-lattice and bullet-lattice interactions. These potentials start at $0.01a_H$ (a_H = Bohr radius = 0.529Å) and are spaced every $0.01a_H$ up to $5.0a_H$ interatomic separation. Secondly, a control card associated with each deck of potentials is read. This control card allows the extrapolation of a Born-Mayer type potential (if desired) from any point on the Interaction Potential Function Curve. Thirdly, the potential at the nearest neighbor distance is determined and then the potential is zeroed at that distance. All potentials at atomic separations smaller than the nearest neighbor distance are adjusted accordingly. All potentials at separations larger than the nearest neighbor distances were set equal to zero. This does not leave any potential free regions in the lattice. Fourthly, potentials are converted to electron volts. Finally, the relation between the force and potential energy can be expressed simply as

$$F(X) = -\nabla U(X).$$

Assuming that the potential is linear between any two successive points in the potential table, the force can be expressed simply as

$$\text{Force} = (U(X) - U(X + \Delta))\cdot(\text{const})$$

where the constant converts the force to proper units.

The determination of a force or potential from the tables is just a simple matter of interpolation. For example, if the atomic separation between two atoms is $1.275a_H$ one would just make a linear interpolation between the values at $1.27a_H$ and $1.28a_H$. These tables are used in both SUBROUTINE STEP which calculates forces and SUBROUTINE IONPE which calculates potential between the ion and the atoms.

Two points should be noted. First, the nearest neighbor separation is approximately $4.436a_H$. Therefore, for a separation of $4.434a_H$ the interpolation is between the value in the table at $4.43a_H$ and the value at $4.436a_H$. Secondly, the average force between two points is assumed to occur halfway between them. The interpolator for the forces accounts for this fact.

One major problem remains unsolved in the construction of the force table (not in the interpolation of forces in SUBROUTINE STEP after the table has been constructed). While the potentials steadily increase as the interatomic distances decrease, the forces in the force table do not monotonically increase with decreasing atomic separation. This is true only when potentials derived from the Interaction Potential Functions are used. No difficulty arises in the region where a Born-Mayer type of exponential fit for the potentials is made. Here the forces behave as expected.

The reason for this discrepancy is found in the calculation of the interaction potentials that are used by the computer program as data. The interaction potential is calculated exactly from 0.01 to $0.20a_H$ and every $0.20a_H$ to $5.0a_H$ (i.e. 0.2, 0.4, $0.6a_H$ would be calculated exactly, $0.50a_H$ would not). Potentials in between these values are calculated by linear interpolation. Hence, the forces in the table would remain essentially constant in the region where the potentials were derived by linear interpolation and would only change abruptly when a point is reached where the potential was calculated exactly. Thus while the overall force would increase as interatomic separation decreased there would be regions where the force stayed essentially constant or even decreased with decreasing atomic separation.

Two main efforts were made to eliminate this discrepancy both of which began by considering only the potentials that were calculated exactly and discarding those that were determined by linear interpolation. First, subroutine ALI and ATSE from the scientific subroutine package of IBM were used to fit known potentials with a polynomial and using this polynomial, points in between the known potentials were interpolated. In the second method an exponential fit of the known potentials was made, and an interpolator constructed as follows. Assume the potential P at two points x_1 and x_2 are known and are to be joined by an exponential. We desire to know the potential at x_a.

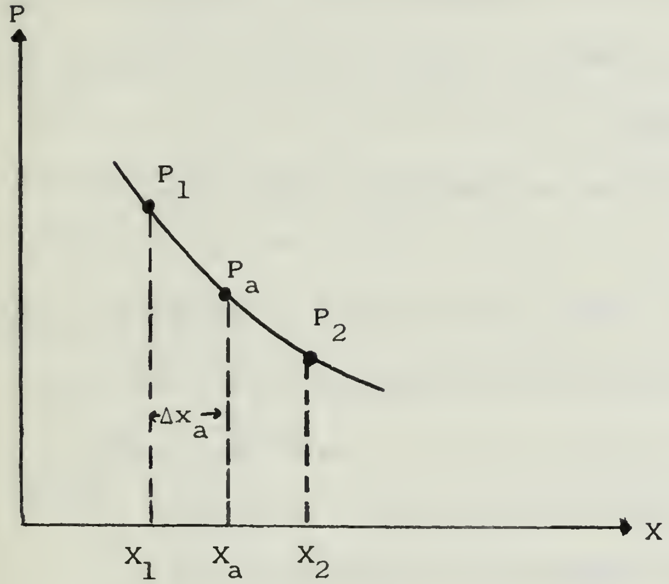

$\Delta X = \frac{X_2 - X_1}{N}$ where N is an integer

(1) $P_1 = A\exp(-Bx_1)$

(2) $P_a = A\exp(-B(x_1+x_a))$ or $P_a = P_1 \exp(-Bx_a)$

Similarly

(3) $P_2 = P_1\exp(-BN\Delta X)$ or $\ln(P_2/P_1) = -B\cdot N\Delta X)$

(4) $B\Delta X = -\ln(P_2/P_1))/N$

Assume $X_a = M\cdot X$ where M is a constant $0 \leq M \leq N$ then

$$P_a = P_1 \exp(-B\Delta X\cdot M)$$

Both the polynomial and exponential fit of known potential yielded approximately the same results. In general, for atomic separations of less than $1.6a_H$ the forces increase with decreasing atomic separation as desired. For separations greater than $1.6a_H$ the forces act as expected, except that in the immediate vicinity ($\sim .02a_H$) of a calculated potential the forces decrease slightly and then increase again. Since there was little to choose between the two methods, the exponential interpolator was selected. The interpolator constructs the tables slightly faster (~ 2 secs) and requires less storage space.

The effects of this problem on the force tables are as follows:

a) Xe^{+6}-Si^{+4}-no effect. The forces behave as expected since the Born-Mayer approximation is constructed beginning at $1.2a_H$.

b) Si^{+4}-Si^{+4} (used as bullet-lattice interaction potential in preliminary studies of (100) channeling). No effect, as a Born-Mayer approximation is constructed beginning at $1.2a_H$.

c) Si^{+1}-Si^{+1} (used as lattice-lattice interactions for all directions of channeling). This force table contains the error discussed above for interatomic separations between 1.4 and $3.0a_H$. However, this error has negligible effect on calculated channeled ranges since (a) there is no error in the force table at atomic separations of $4.4a_H$, the approximate nearest neighbor distance silicon atoms and (b) the bullet passes the lattice atoms so quickly that when two lattice atoms have an interatomic spacing of less than $3.0a_H$ the bullet is no longer under their influence.

While this error in the force table has virtually no effect on channeling range estimates, before the force table concept is used for other computer studies this problem must be solved.

APPENDIX C (PROGRAM PARAMETERS)

The following parameters have been added to the basic computer channeling model (Chan 69MODO).

BPNT - Bullet-Lattice Potential Energy

TPNT - Lattice-Lattice Potential Energy

BFORCE - Bullet-Lattice Force

TFORCE - Lattice-Lattice Force

KA - an integer constant which identifies the point in the potential table where a Born-Mayer potential of form, Ae^{-Bx}, begins

BPCNST - the value of B in the Born-Mayer Potential approximation for the Bullet-Lattice Potentials

TPCNST - the value of B in the Born-Mayer Potential approximation for the Lattice-Lattice Potential

ICHECK, ICOUNT, NCOUNT - constants used in the exponential interpolator between calculated interactions potentials in constructing the Potential Tables

BDELX - a variable ($B\Delta X$) (see appendix II) used in the exponential interpolator between interaction potentials in constructing the Potential Table

ITITLE - 80 alpha numeric characters used on a heading card for potential data deck

LCUT - integer constant with value of either 0 or 1. Used to determine which atoms are in the core (0) or shell (1) of the crystal

CVEDA - conversion factor used to convert electron volts per Bohr to newtons per meter

CLU - conversion factor used to convert distances in LU to distances in units of $100a_H$

AFC - distance in $100a_H$

IFC - integer value of AFC

CLU, AFC, and IFC are used in the following way. Assume interatomic spacing between atoms = 0.5LU

AFC = (CLU) x (DIST) = 256.14

IFC = 256

An AFC of 256.14 corresponds to $2.5614a_H$

An IFC of 256 corresponds to $2.56a_H$

AFC1 - nearest neighbor distance in units of $100a_H$

AFC2 - the reciprocal of the difference between the nearest neighbor distance and 443.0. Used in Subroutines STEP and IONPE.

DFF1 - the difference in $100a_H$ between the atomic separations of the bullet and lattice atom and the nearest neighbor distance of silicon

GETIME, SETIME - machine subroutines used to determine actual program running time. They terminate program execution and have cards punched before exceeding the running time allocated to the program by the computer. This allows a restart capability.

```
********************  SUBROUTINE DL100  *********************
*  THIS IS A LATTICE GENERATOR FOR THE DIAMOND LATTICE IN   *
*  THE (100) ORIENTATION.                                   *
*  THE CRYSTAL DEVELOPS IN THE ORDER X,FOLLOWED BY Z,       *
*  FOLLOWED BY Y                                            *
*************************************************************
      COMMON/COM1/RX(200),RY(200),RZ(200),LCUT(200),LL,LD
      COMMON/COM2/ROF,ROF2,ROFM,AC,PAC,PPTC,PTC,PFPTC,FPTC,
     2 FM,PFIV,TPOT
      COMMON/COM4/IX,IY,IZ,IXP,IYP,IZP,SCX,SCY,SCZ,IDEEP
      COMMON/COM7/R1,LSS,SPX,SPZ,COX,COY,COZ
      COMMON/COM9/ IDX,IDY,IDZ(200),DXT,DYT,DZT,TPOX,TPOY,
     2 TPOZ
      COMMON/COM22/XLL,XLF,ZLL,ZLF
*************************************************************
*  THE FOLLOWING CONSTANTS ARE USED EITHER BY THIS SUB-     *
*  ROUTINE TO GENERATE THE LATTICE OR IN OTHER SUBROUTINES  *
*  AS REQUIRED.                                             *
*************************************************************
      XLL=0.99
      XLF=3.01
      ZLL=0.99
      ZLF=3.01
      M=2
      LA=2
      IB=1
      IDX=1
      IDY=41
      IX=5
      IY=5
      IZ=5
      SCX=1.0
      SCY=1.0
      SCZ=1.0
      DXT=2.0*SCX
      DYT=2.0*SCY
      DZT=2.0*SCZ
      DY=0.5
      DX=0.5
      DZ=0.5
*************************************************************
*  THE FOLLOWING SERIES OF NESTED DO LOOPS GENERATE THE     *
*  LATTICE AND INSURE IT CONTAINS THE REQUIRED SYMMETRY     *
*************************************************************
      JT=0
      Y=-SCY
      DO 60 J=1,IY
      Y=Y+SCY
      KT=0
      Z=-SCZ
      DO 50 K=1,IZ
      Z=Z+SCZ
      IT=0
      X=-SCX
      DO 40 I=1,IX
      X=X+SCX
      ITT=IT+JT+KT
      IF(ITT-(ITT/2*2)) 40,30,40
   30 RX(M)=X
      RY(M)=Y
      RZ(M)=Z
      IDZ(M)=5
      L=M
      M=M+1
   40 IT=IT+1
   50 KT=KT+1
      IF(J.EQ.5) GO TO 80
      DO 200 IA=LA,L
      IF(4.0*SCX-RX(IA)*SCX) 200,200,202
  202 IF(4.0*SCZ-RZ(IA)*SCZ) 200,200,203
  203 RX(L+IB)=RX(IA)+DX
      RY(L+IB)=RY(IA)+DY
      RZ(L+IB)=RZ(IA)+DZ
      IDZ(L+IB)=4
      IB=IB+1
  200 CONTINUE
      M=L+9
      LA=M
      IB=1
   60 JT=JT+1
   80 LL=M-1
************************************************************
*  THE FOLLOWING DO LOOP DIVIDES THE CRYSTAL INTO AN ACTIVE*
*  CORE AND AN INACTIVE SURROUNDING SHELL.                 *
************************************************************
      DO 2 I=2,LL
      LCUT(I)=0
      IF(RX(I).GT.3.1.OR.RX(I).LT.0.9) LCUT(I)=1
      IF(RY(I).GT.2.5) LCUT(I)=1
      IF(RZ(I).LE.0.9.OR.RZ(I).GE.3.1) LCUT(I)=1
    2 CONTINUE
      LCUT(1)=0
      R1=(ROE+RY(2))/ABS(COY)
      RETURN
      END
```

Computer Program - SUBROUTINE DL110

```
********************  SUBROUTINE DL110  *********************
*  THIS IS A LATTICE GENERATOR FOR THE DIAMOND LATTICE IN   *
*  THE (110) ORIENTATION.                                    *
*  THE CRYSTAL DEVELOPS IN THE ORDER X,FOLLOWED BY Z,        *
*  FOLLOWED BY Y                                             *
*************************************************************
      COMMON/COM1/RX(200),RY(200),RZ(200),LCUT(200),LL,LD
      COMMON/COM2/ROE,ROE2,ROEM,AC,RAC,PETC,PTC,PEPTC,EPTC,
     2 EM,REIV,TROT
      COMMON/COM4/IX,IY,IZ,IXP,IYP,IZP,SCX,SCY,SCZ,IDEEP
      COMMON/COM7/R1,LSS,SPX,SPZ,COX,COY,COZ
      COMMON/COM9/ IDX,IDY,IDZ(200),DXT,DYT,DZT,TPOX,TPOY,
     2 TPOZ
      COMMON/COM22/XLL,XLE,ZLL,ZLE
*************************************************************
*  THE FOLLOWING CONSTANTS ARE USED EITHER BY THIS SUB-     *
*  ROUTINE TO GENERATE THE LATTICE OR IN OTHER SUBROUTINES  *
*  AS REQUIRED.                                              *
*************************************************************
      XLL=0.697
      XLE=2.131
      ZLL=0.99
      ZLE=3.01
      M=2
      IDX=1
      IDY=23
      IX=5
      IY=5
      IZ=5
      RO=1.0/SQRT(2.0)
      SCX=RO
      SCY=RO
      SCZ=1.0
      DXT=2.0*SCX
      DYT=2.0*SCY
      DZT=2.0*SCZ
      DX=RO
      DY=0.0
      DZ=0.5
*************************************************************
*  THE FOLLOWING SERIES OF NESTED DO LOOPS GENERATE THE     *
*  LATTICE AND INSURE IT CONTAINS THE REQUIRED SYMMETRY     *
*************************************************************
      JT=0
      Y=-SCY
      DO 60 J=1,IY
      Y=Y+SCY
      KT=0
      Z=-SCZ
      DO 50 K=1,IZ
      Z=Z+SCZ
      IT=0
      X=-SCX
      MA=M
      DO 40 I=1,IX
      X=X+SCX
      IF(IT-(IT/2)*2) 21,11,21
   11 IF(JT-(JT/2)*2) 40,12,40
   12 IF(KT-(KT/2)*2) 40,30,40
   21 IF(JT-(JT/2)*2) 22,40,22
   22 IF(KT-(KT/2)*2) 30,40,30
   30 RX(M)=X
      RY(M)=Y
      RZ(M)=Z
      L=M
      M=M+1
   40 IT=IT+1
      MB=M-1
      IF(MB-MA) 210,210,198
  198 IF(JT.EQ.1) GO TO 215
      IF(JT.EQ.3) GO TO 215
  199 DO 200 I=MA,MB
      IF(3.9*SCX-RX(I)) 200,200,202
  202 IF(4.0*SCZ-RZ(I)) 200,200,203
  203 RX(M)=RX(I)+DX
      RY(M)=RY(I)+DY
      RZ(M)=RZ(I)+DZ
      M=M+1
  200 CONTINUE
      GO TO 210
  215 LR=M-2
      RX(M)=RX(LR)-DX
      RY(M)=RY(LR)+DY
      RZ(M)=RZ(LR)+DZ
      M=M+1
      GO TO 199
  210 CONTINUE
   50 KT=KT+1
   60 JT=JT+1
      LL=M-1
      DO 2 I=2,LL
    2 IDZ(I)=5
************************************************************
*  THE FOLLOWING DO LOOP DIVIDES THE CRYSTAL INTO AN ACTIVE*
*  CORE AND AN INACTIVE SURROUNDING SHELL.                 *
************************************************************
      DO 9 I=2,LL
      LCUT(I)=0
      IF(RY(I).GT.2.2) LCUT(I)=1
      IF(RZ(I).GT.3.9) LCUT(I)=1
      IF(RZ(I).LT.0.4) LCUT(I)=1
    9 CONTINUE
      LCUT(1)=0
      R1=(ROF+RY(2))/ABS(COY)
      RETURN
      END
```

Computer Program - SUBROUTINE DL111

```
********************  SUBROUTINE DL111  **********************
*  THIS IS A LATTICE GENERATOR FOR THE DIAMOND LATTICE IN    *
*  THE (111) ORIENTATION.                                     *
*  THE CRYSTAL DEVELOPS IN THE ORDER X,FOLLOWED BY Z,         *
*  FOLLOWED BY Y                                              *
**************************************************************
      COMMON/COM1/RX(200),RY(200),RZ(200),LCUT(200),LL,LD
      COMMON/COM2/ROE,ROE2,ROEM,AC,PAC,PPTC,PTC,PFPTC,FPTC,
     2 FM,PFIV,TPOT
      COMMON/COM4/IX,IY,IZ,IXP,IYP,IZP,SCX,SCY,SCZ,IDEEP
      COMMON/COM7/R1,LSS,SPX,SPZ,COX,COY,COZ
      COMMON/COM9/ IDX,IDY,IDZ(200),DXT,DYT,DZT,TPOX,TPOY,
     2 TPOZ
      COMMON/COM22/XLL,XLF,ZLL,ZLF,YLL,YLF
**************************************************************
*  THE FOLLOWING CONSTANTS ARE USED EITHER BY THIS SUB-       *
*  ROUTINE TO GENERATE THE LATTICE OR IN OTHER SUBROUTINES   *
*  AS REQUIRED.                                               *
**************************************************************
      XLL=0.697
      XLF=2.131
      YLL=2.5
      YLF=4.4
      ZLL=1.215
      ZLF=3.684
      M=2
      LA=2
      IB=1
      IDX=1
      IDY=66
      DO 2 I=2,150
    2 IDZ(I)=5
      IX=5
      IY=7
      IZ=5
      SCX=1.0/SQRT(2.0)
      SCY=2.0/SQRT(3.0)
      SCZ=SQRT(1.5)
      SSCZ=SCZ/3.0
      DXT=2.0*SCX
      DYT=2.0*SQRT(3.0)
      DZT=2.0*SCZ
      DX=0.0
      DY=SQRT(0.75)
      DZ=0.0
**************************************************************
*  THE FOLLOWING SERIES OF NESTED DO LOOPS GENERATE THE       *
*  LATTICE AND INSURE IT CONTAINS THE REQUIRED SYMMETRY       *
**************************************************************
      JT=0
      Y=-SCY
      DO 60 J=1,IY
      Y=Y+SCY
      KT=0
      JTS=JT+JT/3
      Z=-SCZ
      DO 50 K=1,IZ
      IF(K.EQ.5) GO TO 80
   90 CONTINUE
      Z=Z+SCZ
      IT=0
      X=-SCX
      DO 40 I=1,IX
      X=X+SCX
      IN=IT+JTS+KT
      IF(IN-(IN/2)*2) 40,30,40
   30 RX(M)=X
      RY(M)=Y
      IF(JT-3*(JT/3)) 31,35,31
   31 JTT=JT
   32 JTT=JTT-3
      IF(JTT) 33,35,32
   33 JTT=JTT+3
      ZP=JTT
      RZ(M)=Z+ZP*SSCZ
      GO TO 37
   35 RZ(M)=Z
   37 L=M
      M=M+1
      GO TO 40
   80 IF(J.EQ.1) GO TO 90
      IF(J.EQ.4) GO TO 90
      IF(J.EQ.7) GO TO 90
      GO TO 85
   40 IT=IT+1
   50 KT=KT+1
   85 IF(J.EQ.7) GO TO 100
      MA=0
      DO 200 IA=LA,L
      IF(4.0*SCX-RX(IA)*SCX) 200,200,202
  202 IF(4.0*SCZ-RZ(IA))200,203,203
  203 RX(L+IB)=RX(IA)+DX
      RY(L+IB)=RY(IA)+DY
      RZ(L+IB)=RZ(IA)+DZ
      IB=IB+1
      MA=MA+1
  200 CONTINUE
      M=L+MA+1
      LA=M
      IB=1
   60 JT=JT+1
  100 LL=M-1
************************************************************
*  THE FOLLOWING DO LOOP DIVIDES THE CRYSTAL INTO AN ACTIVE*
*  CORE AND AN INACTIVE SURROUNDING SHELL.                 *
************************************************************
      DO 3 I=2,LL
      LCUT(I)=0
      IF(RX(I).LT.0.7.OR.RX(I).GT.2.2) LCUT(I)=1
      IF(RZ(I).LT.1.4.OR.RZ(I).GT.3.7) LCUT(I)=1
      IF(RY(I).GT.5.2) LCUT(I)=1
    3 CONTINUE
      LCUT(1)=0
      R1=(ROE+RY(2))/ABS(COY)
      RETURN
      END
```

Computer Program - Exponential Interpolator

```
****************  EXPONENTIAL INTERPOLATOR   ****************
*  READ LATTICE-LATTICE POTENTIALS AND DETERMINE IF A BORN-*
*  MAYER APPROXIMATION IS NECESSARY                         *
*************************************************************
      READ(5,9825)(ITITLE(I),I=1,20)
      READ(5,9810)(TPNT(I),I=1,20)
      READ(5,9815)(TPNT(I),I=21,500)
      READ(5,9820)KA,TPCNST
      IF(KA) 405,405,410
  405 ICHECK=460
      GO TO 416
*************************************************************
*  CONSTRUCT A BORN-MAYER POTENTIAL                         *
*************************************************************
  410 DO 415 I=KA,500
  415 TPNT(I)=TPNT(KA)*EXP(TPCNST*((I/100.)-(KA/100.)))
*************************************************************
*  MAKE AN EXPONENTIAL INTERPOLATION BETWEEN CALCULATED     *
*  POTENTIALS                                               *
*************************************************************
      ICHECK=KA
  416 ICOUNT=20
  417 DO 419 I=1,20
      NCOUNT=ICOUNT+20
      BDELX=-ALOG(TPNT(NCOUNT)/TPNT(ICOUNT))/20.
  419 TPNT(ICOUNT+I)=TPNT(ICOUNT)*EXP((-I)*BDELX)
      IF(ICHECK-NCOUNT) 422,422,421
  421 ICOUNT=NCOUNT
      GO TO 417
*************************************************************
*  DETERMINE POTENTIAL AT NEAREST NEIGHBOR DISTANCE,ZERO    *
*  POTENTIAL TABLE,AND CONVERT POTENTIAL TO ELECTRON VOLTS *
*************************************************************
  422 TTPNT=TPNT(IFC)+((TPNT(IFC+1)-TPNT(IFC))*(AFC-IFC))
      DO 420 I=1,500
      TPNT(I)=(TPNT(I)-TTPNT)*13.6
      IF(TPNT(I))425,420,420
  425 TPNT(I)=0.0
  420 CONTINUE
*************************************************************
*  CONSTRUCT A LATTICE-LATTICE FORCE TABLE                  *
*************************************************************
      DO 430 I=1,499
  430 TFORCE(I)=(TPNT(I)-TPNT(I+1))*CVEDA
*************************************************************
*  READ BULLET-LATTICE POTENTIALS AND DETERMINE IF A BORN-  *
*  MAYER APPROXIMATION IS NECESSARY                         *
*************************************************************
      READ(5,9825)(ITITLE(I),I=21,40)
      READ(5,9810)(BPNT(I),I=1,20)
      READ(5,9815)(BPNT(I),I=21,500)
      READ(5,9820)KA,BPCNST
      IF(KA) 445,445,450
  445 ICHECK=460
      GO TO 456
*************************************************************
*  CONSTRUCT A BORN-MAYER POTENTIAL                         *
*************************************************************
  450 DO 455 I=KA,500
  455 BPNT(I)=BPNT(KA)*EXP(BPCNST*((I/100.)-(KA/100.)))
*************************************************************
*  MAKE AN EXPONENTIAL INTERPOLATION BETWEEN CALCULATED     *
*  POTENTIALS                                               *
*************************************************************
      ICHECK=KA
  456 ICOUNT=20
  457 DO 459 I=1,20
      NCOUNT=ICOUNT+20
      BDELX=-ALOG(BPNT(NCOUNT)/BPNT(ICOUNT))/20.
  459 BPNT(ICOUNT+I)=BPNT(ICOUNT)*EXP((-I)*BDELX)
      IF(ICHECK-NCOUNT) 462,462,461
  461 ICOUNT=NCOUNT
      GO TO 457
************************************************************
*  DETERMINE POTENTIAL AT NEAREST NEIGHBOR DISTANCE,ZERO   *
*  POTENTIAL TABLE,AND CONVERT POTENTIAL TO ELECTRON VOLTS *
************************************************************
  462 BBPNT=BPNT(IFC)+((BPNT(IFC+1)-BPNT(IFC))*(AFC-IFC))
      DO 480 I=1,500
      BPNT(I)=(BPNT(I)-BBPNT)*13.6
      IF(BPNT(I))475,480,480
  475 BPNT(I)=0.0
  480 CONTINUE
************************************************************
*  CONSTRUCT A BULLET-LATTICE FORCE TABLE                  *
************************************************************
  485 DO 490 I=1,499
  490 BFORCE(I)=(BPNT(I)-BPNT(I+1))*CVEDA
******************  END OF INTERPOLATOR  *******************
```

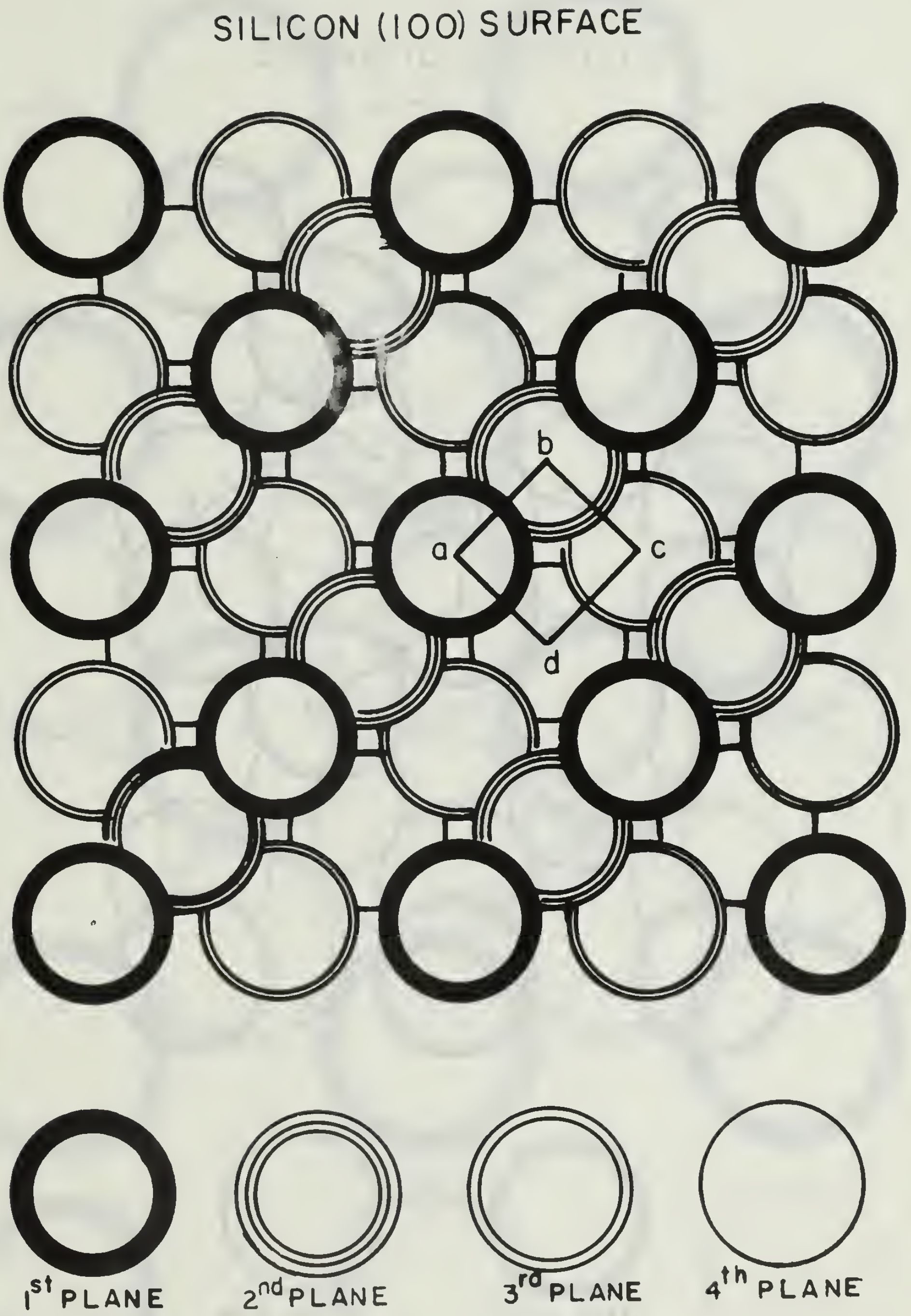
SILICON (100) SURFACE
b
a
c
d
1st PLANE
2nd PLANE
3rd PLANE
4th PLANE

Figure 1.

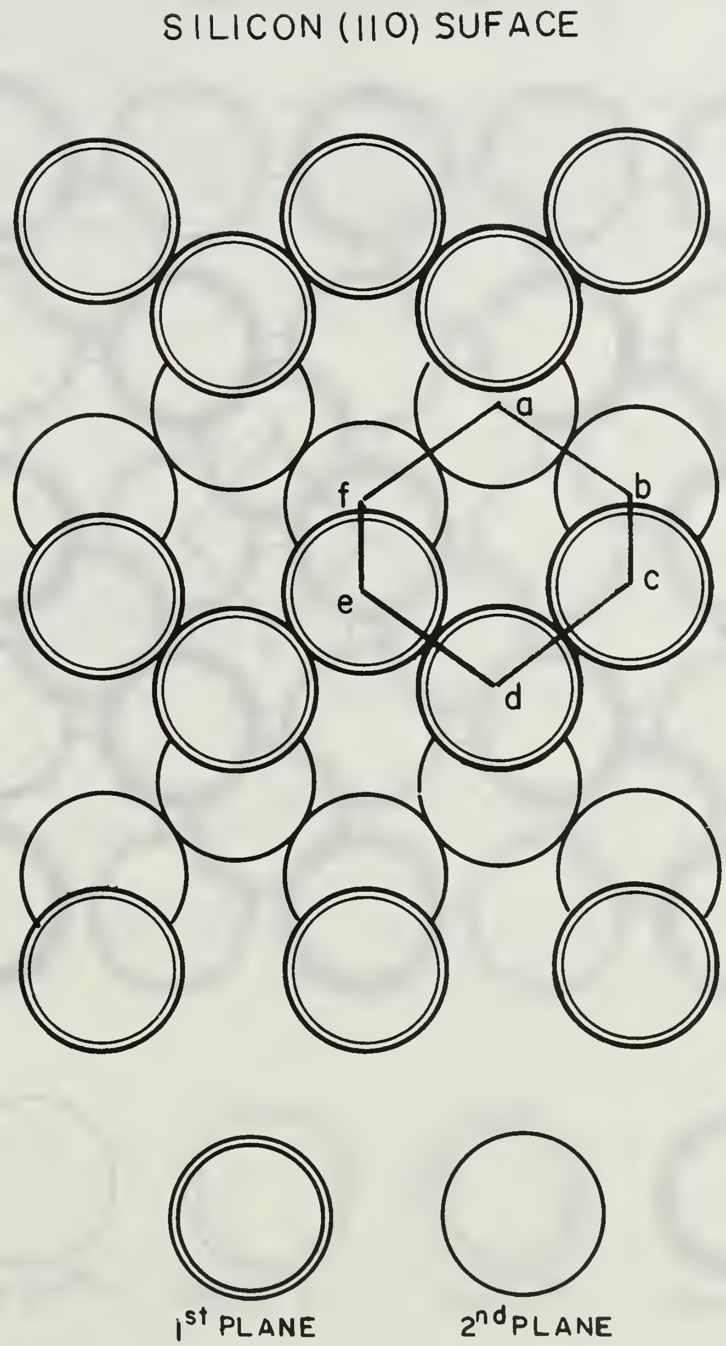

SILICON (110) SUFACE

Figure 2.

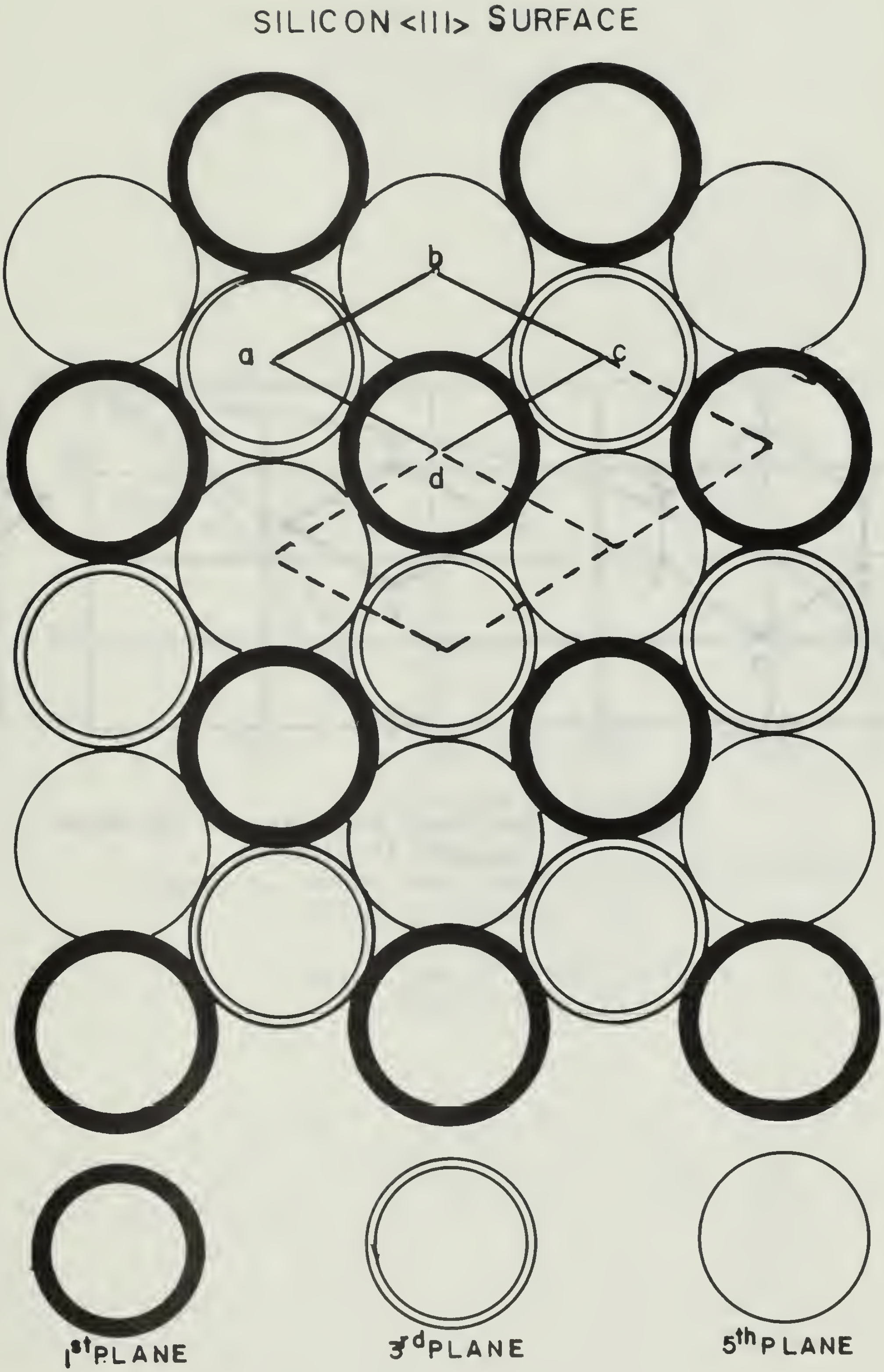

Figure 3.

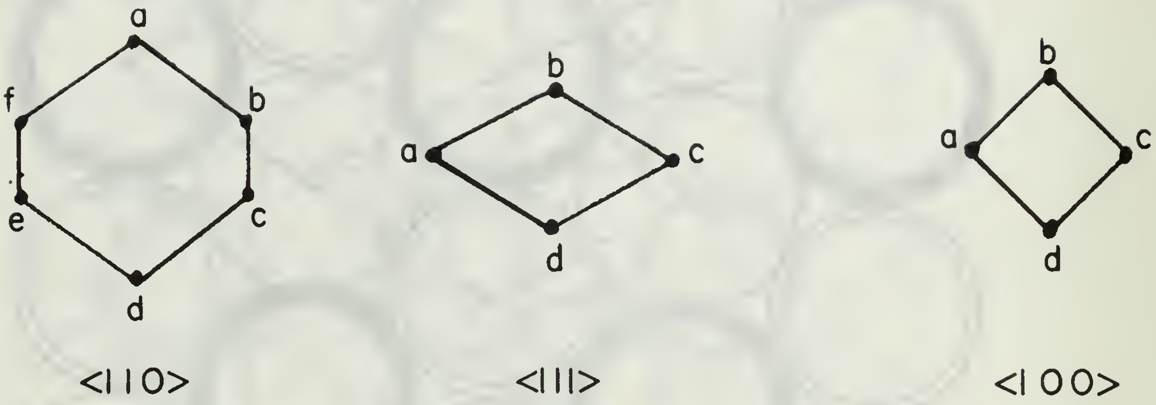

<110>   <111>   <100>

Figure 4. The shape and sizes of the major channels in silicon.

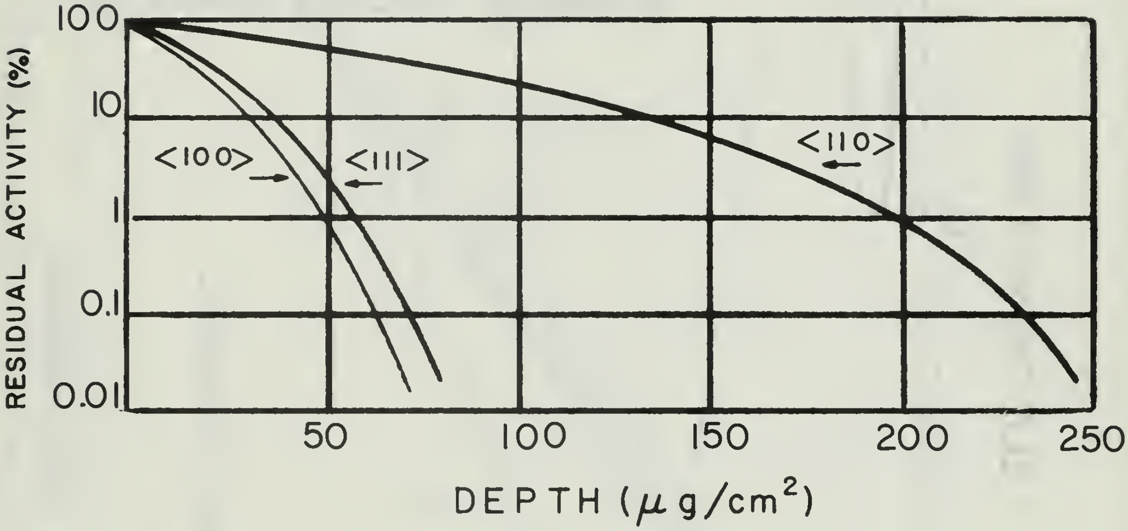

Figure 5. Range distribution curves for 40 KeV ^{125}Xe in silicon.

Note: $1\mu g/cm^2 = 42Å = 15.5LU$.
(Ref 1, Fig. 5)

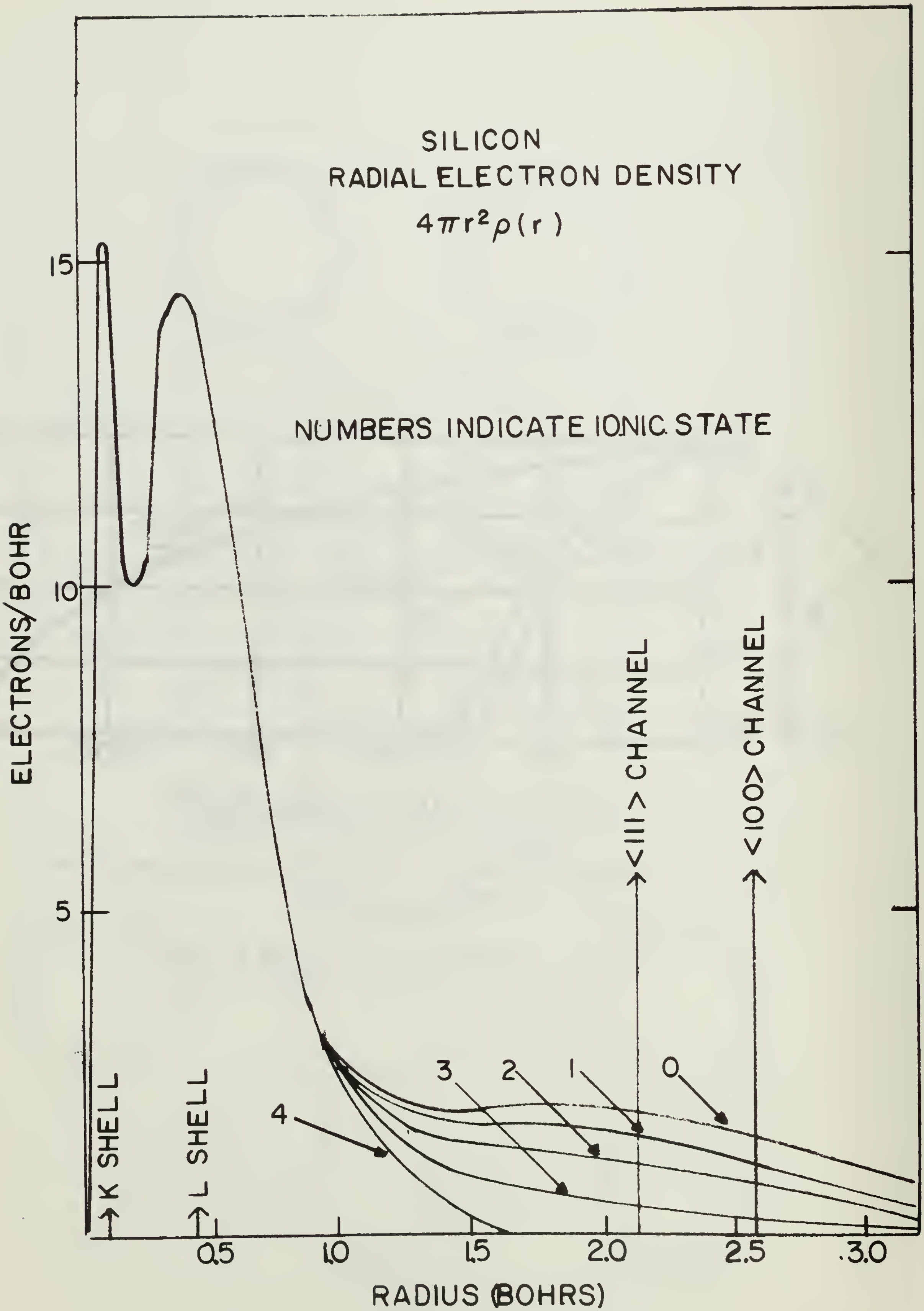
SILICON
RADIAL ELECTRON DENSITY
$4\pi r^2\rho(r)$
NUMBERS INDICATE IONIC STATE
ELECTRONS/BOHR
15
10
5
<111> CHANNEL
<100> CHANNEL
K SHELL
L SHELL
0
1
2
3
4
0.5
1.0
1.5
2.0
2.5
3.0
RADIUS (BOHRS)

Figure 6.

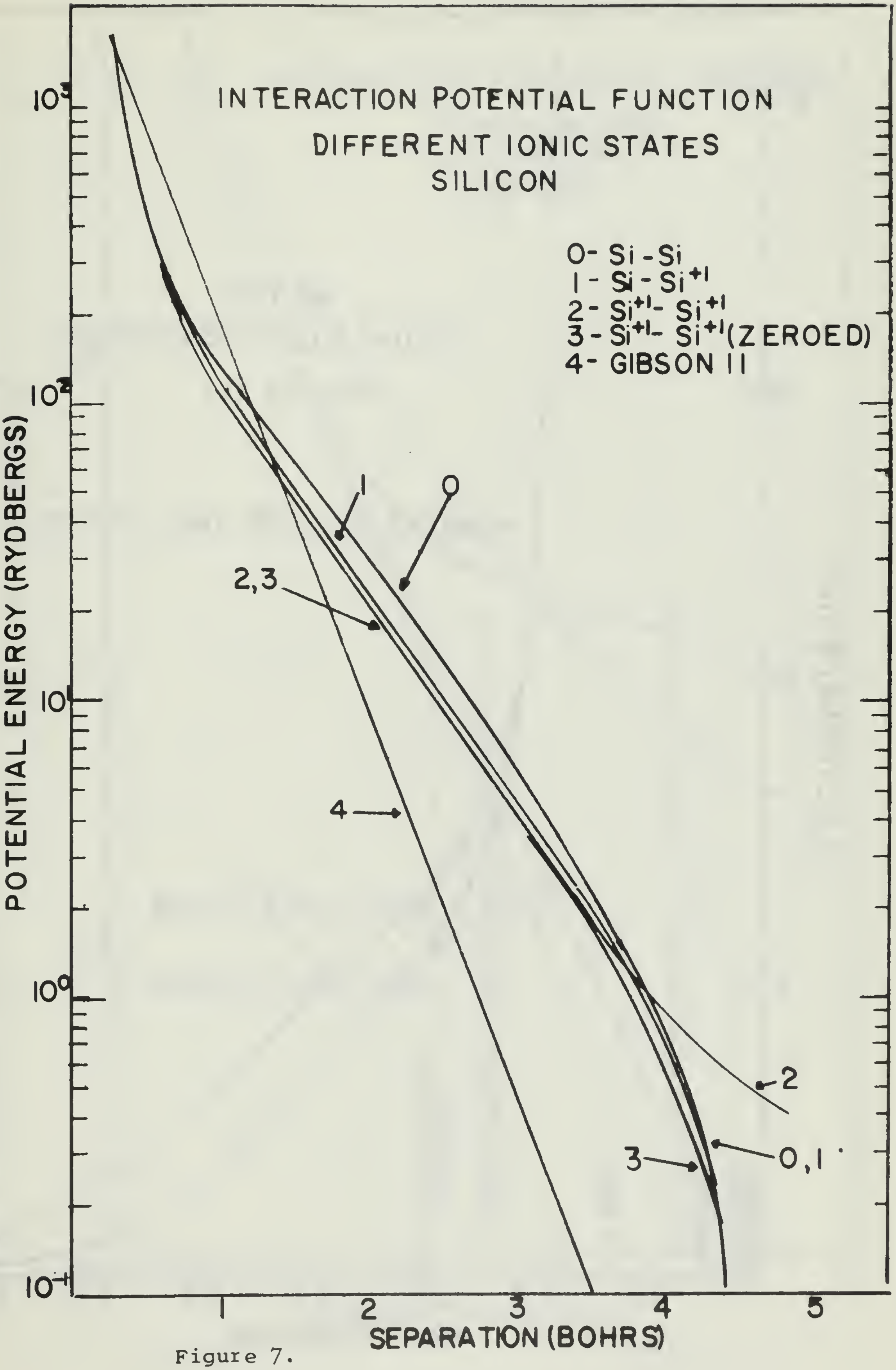
INTERACTION POTENTIAL FUNCTION
DIFFERENT IONIC STATES
SILICON
0- Si-Si
1- Si-Si^{+1}
2- Si^{+1}- Si^{+1}
3- Si^{+1}- Si^{+1}(ZEROED)
4- GIBSON II
10^3
10^2
10^1
10^0
10^{-1}
1
0
2,3
4
2
3
0,1
1
2
3
4
5
POTENTIAL ENERGY (RYDBERGS)
SEPARATION (BOHRS)

Figure 7.

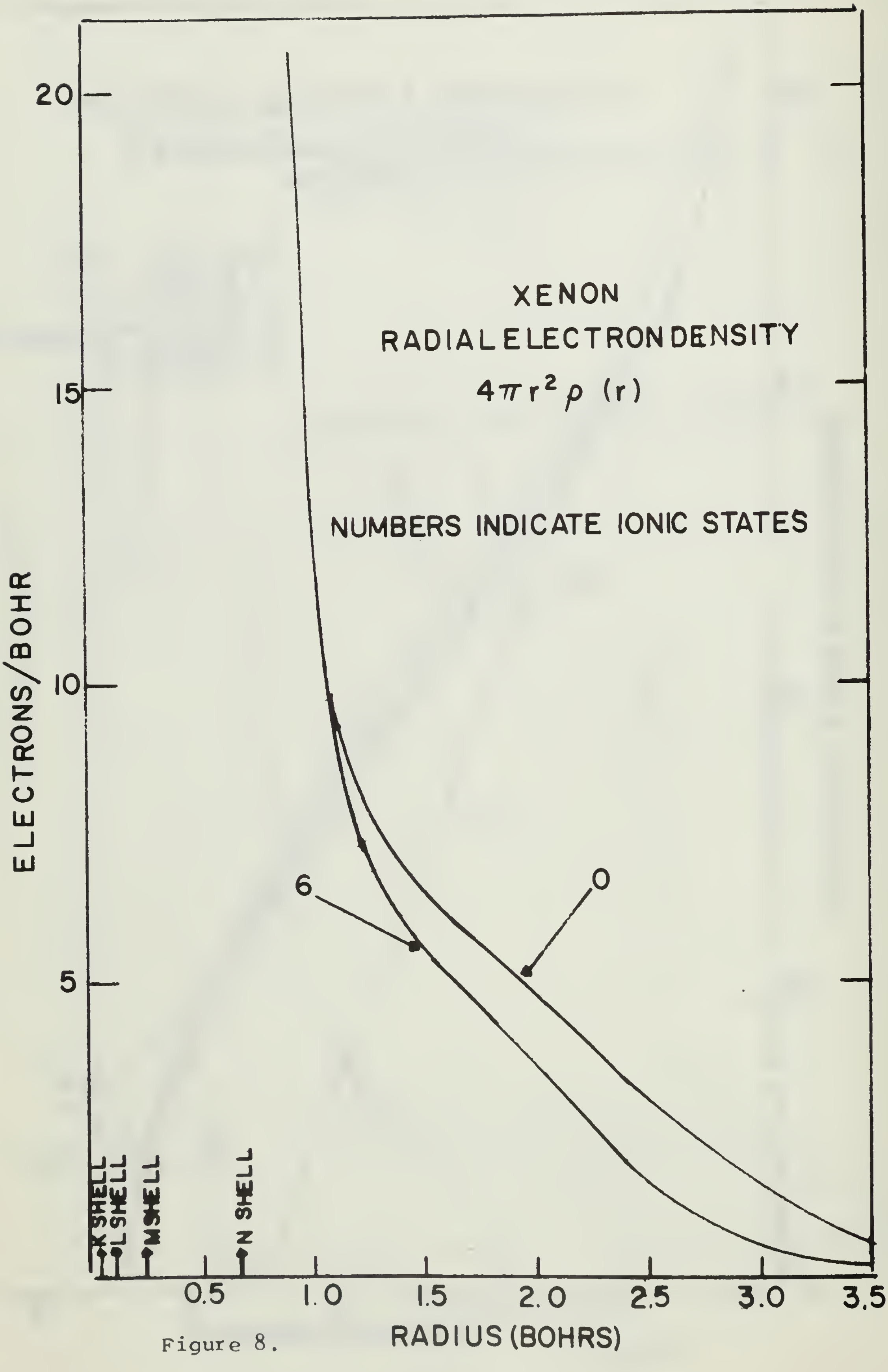
XENON
RADIAL ELECTRON DENSITY
$4\pi r^2 \rho (r)$
NUMBERS INDICATE IONIC STATES
6
0
ELECTRONS/BOHR
20
15
10
5
K SHELL
L SHELL
M SHELL
N SHELL
0.5
1.0
1.5
2.0
2.5
3.0
3.5
RADIUS (BOHRS)

Figure 8.

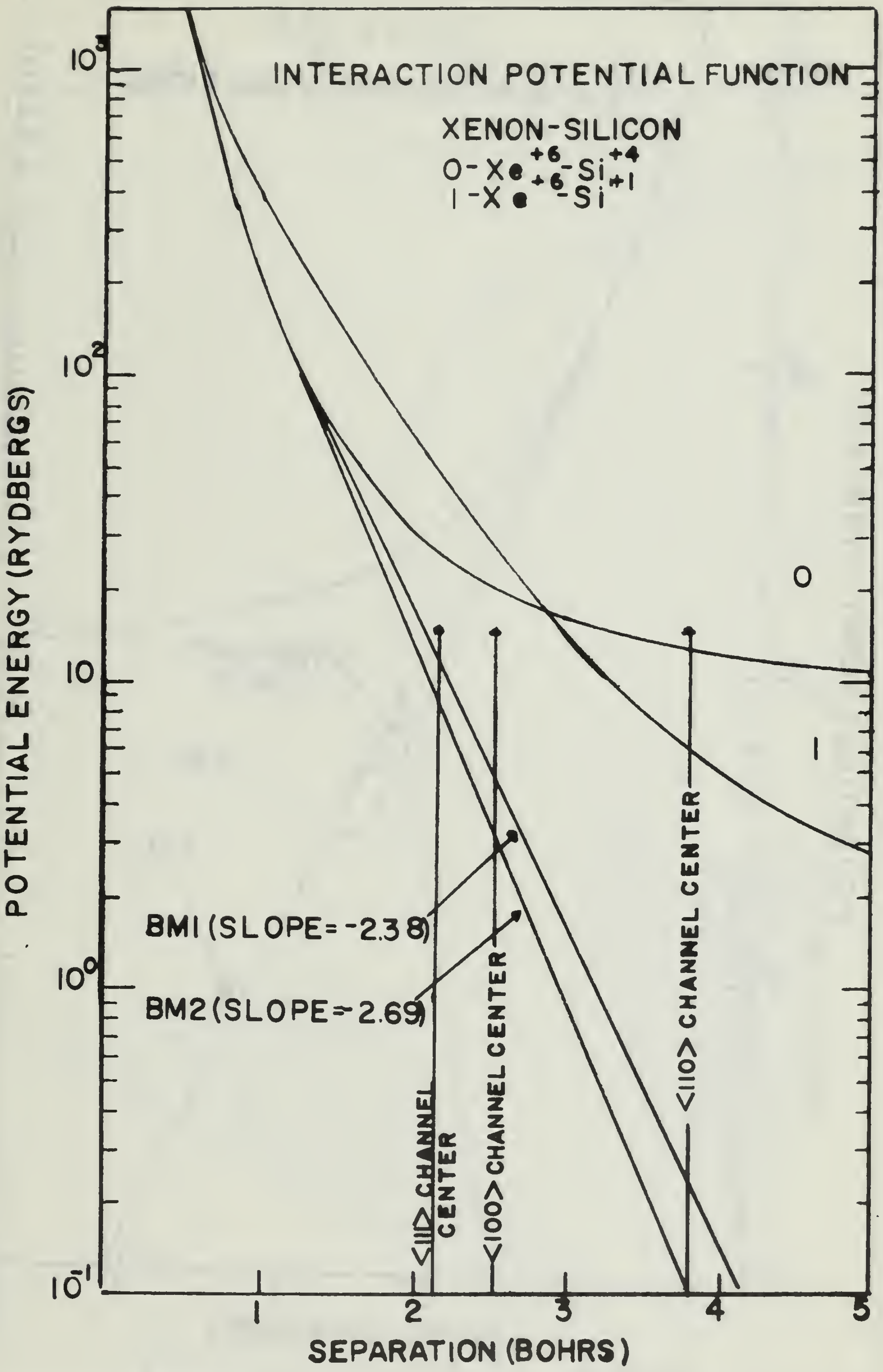
INTERACTION POTENTIAL FUNCTION
XENON-SILICON
O-Xe^{+6}-Si^{+4}
1-Xe^{+6}-Si^{+1}
O
1
BM1 (SLOPE=-2.38)
BM2 (SLOPE=-2.69)
<111> CHANNEL CENTER
<100> CHANNEL CENTER
<110> CHANNEL CENTER
10^3
10^2
10
10^0
10^{-1}
1
2
3
4
5
POTENTIAL ENERGY (RYDBERGS)
SEPARATION (BOHRS)

Figure 9.

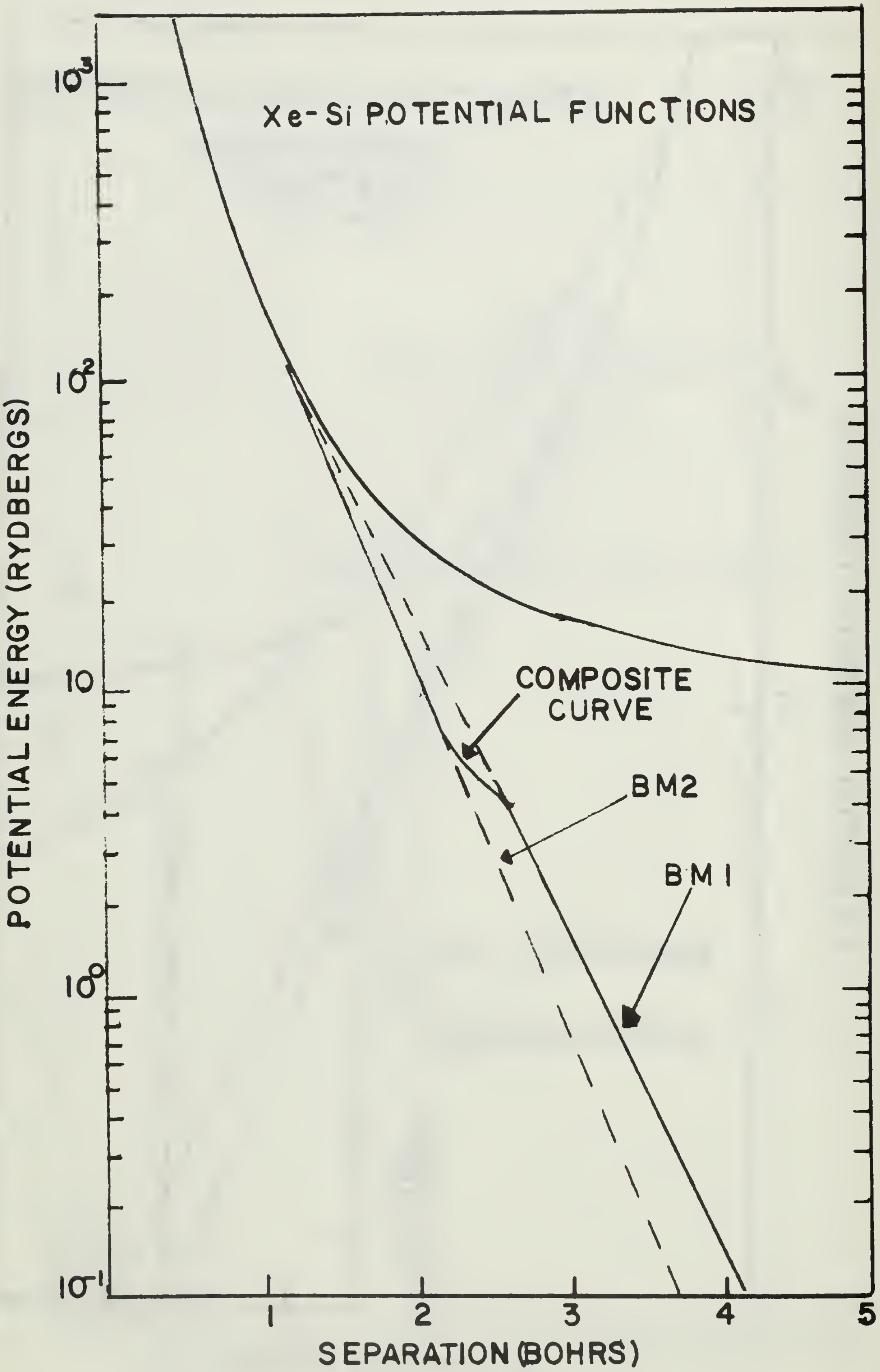
Xe-Si POTENTIAL FUNCTIONS
POTENTIAL ENERGY (RYDBERGS)
SEPARATION (BOHRS)
10^3
10^2
10
10^0
10^{-1}
1
2
3
4
5
COMPOSITE CURVE
BM2
BM1

Figure 10.

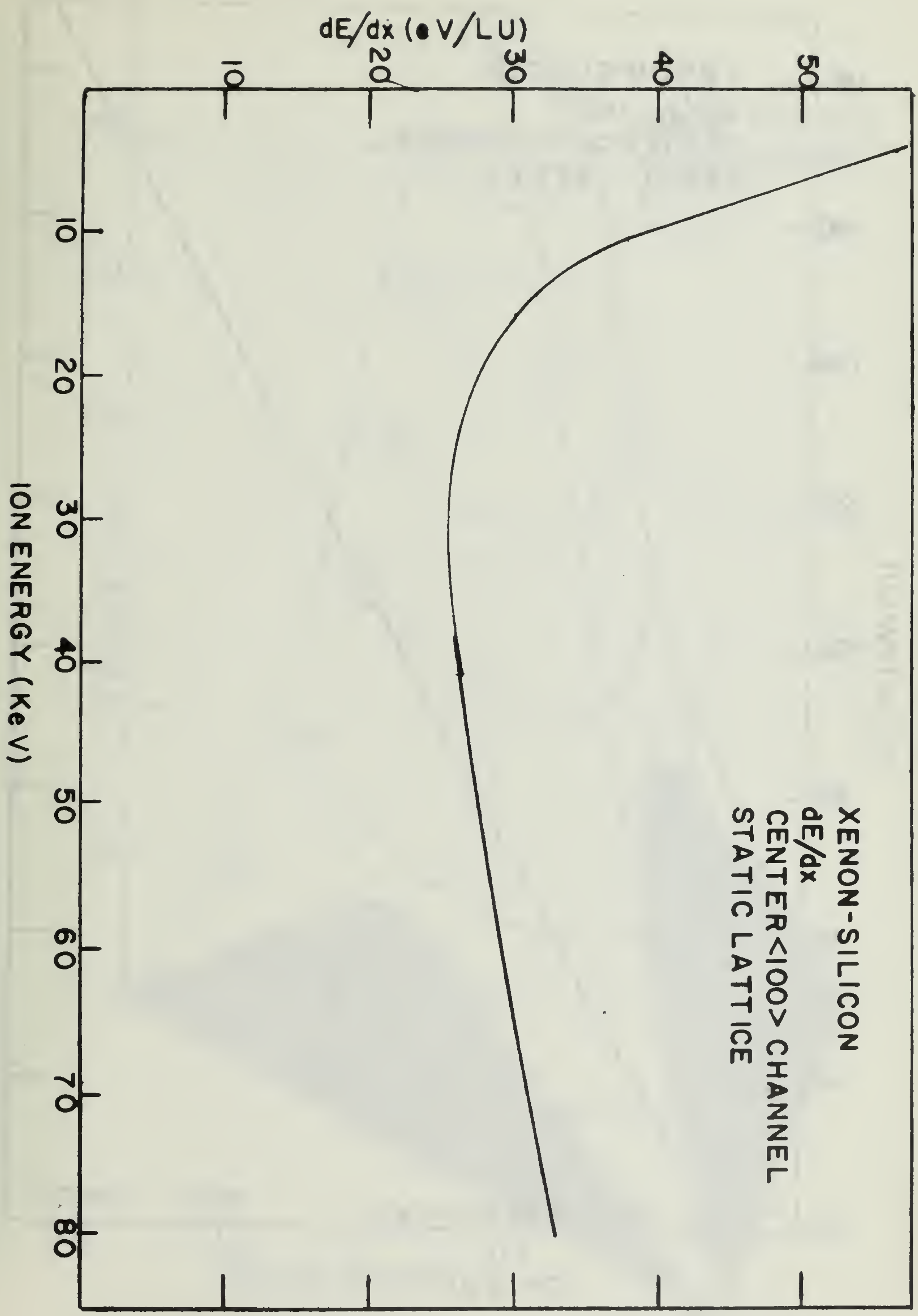
dE/dx (eV/LU)
10
20
30
40
50
10
20
30
40
50
60
70
80
ION ENERGY (KeV)
XENON-SILICON
dE/dx
CENTER<100> CHANNEL
STATIC LATTICE

Figure 11.

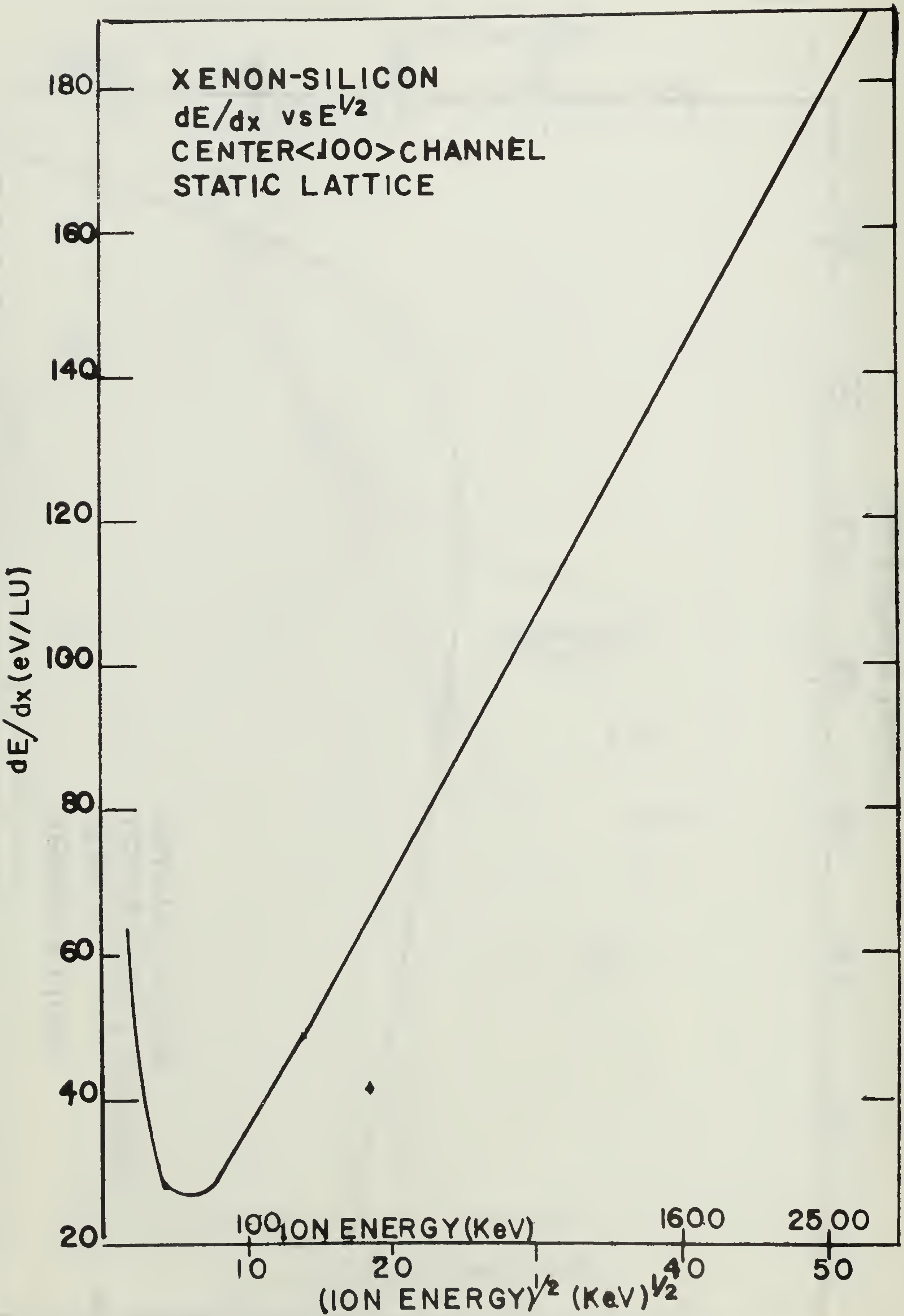
XENON-SILICON
dE/dx vs E^1/2
CENTER<100>CHANNEL
STATIC LATTICE
dE/dx (eV/LU)
180
160
140
120
100
80
60
40
20
100
ION ENERGY(KeV)
1600
2500
10
20
40
50
(ION ENERGY)^1/2 (KeV)^1/2

Figure 12.

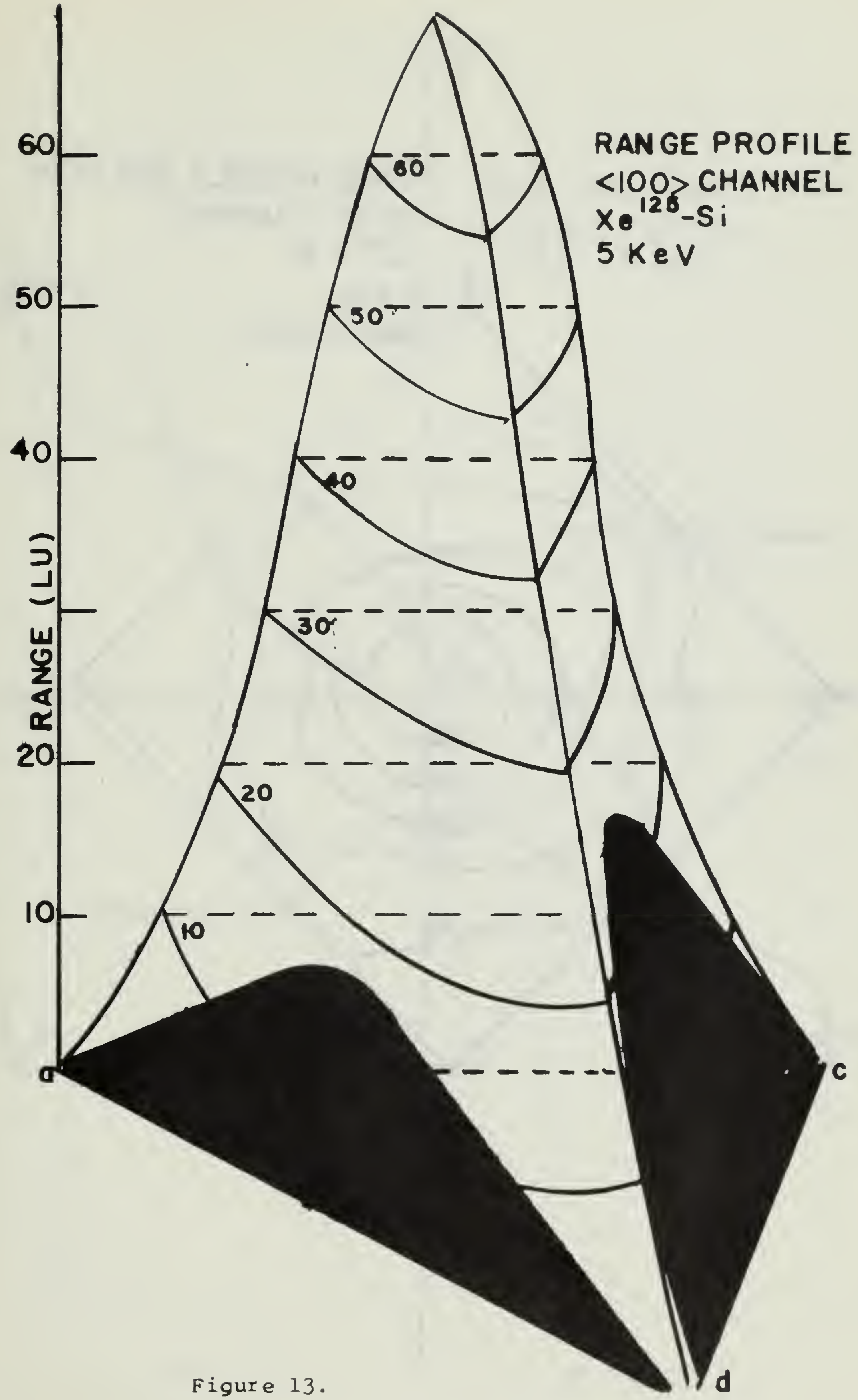
RANGE PROFILE
<100> CHANNEL
Xe^{128}-Si
5 KeV
RANGE (LU)
60
50
40
20
10
60
50
40
30
20
10
a
c
d

Figure 13.

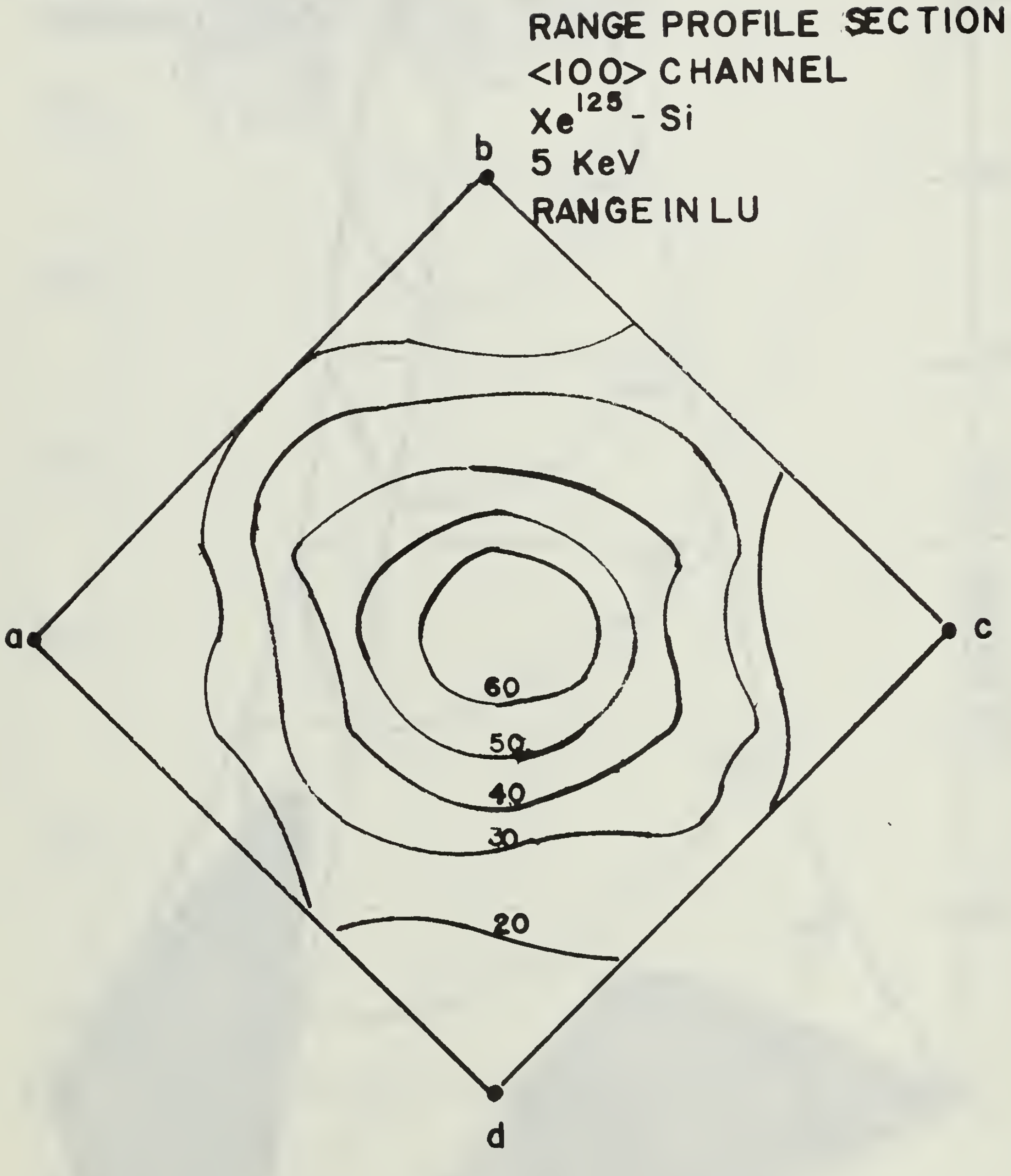
RANGE PROFILE SECTION
<100> CHANNEL
Xe^{125} - Si
5 KeV
RANGE IN LU
a
b
c
d
60
50
40
30
20

Figure 14.

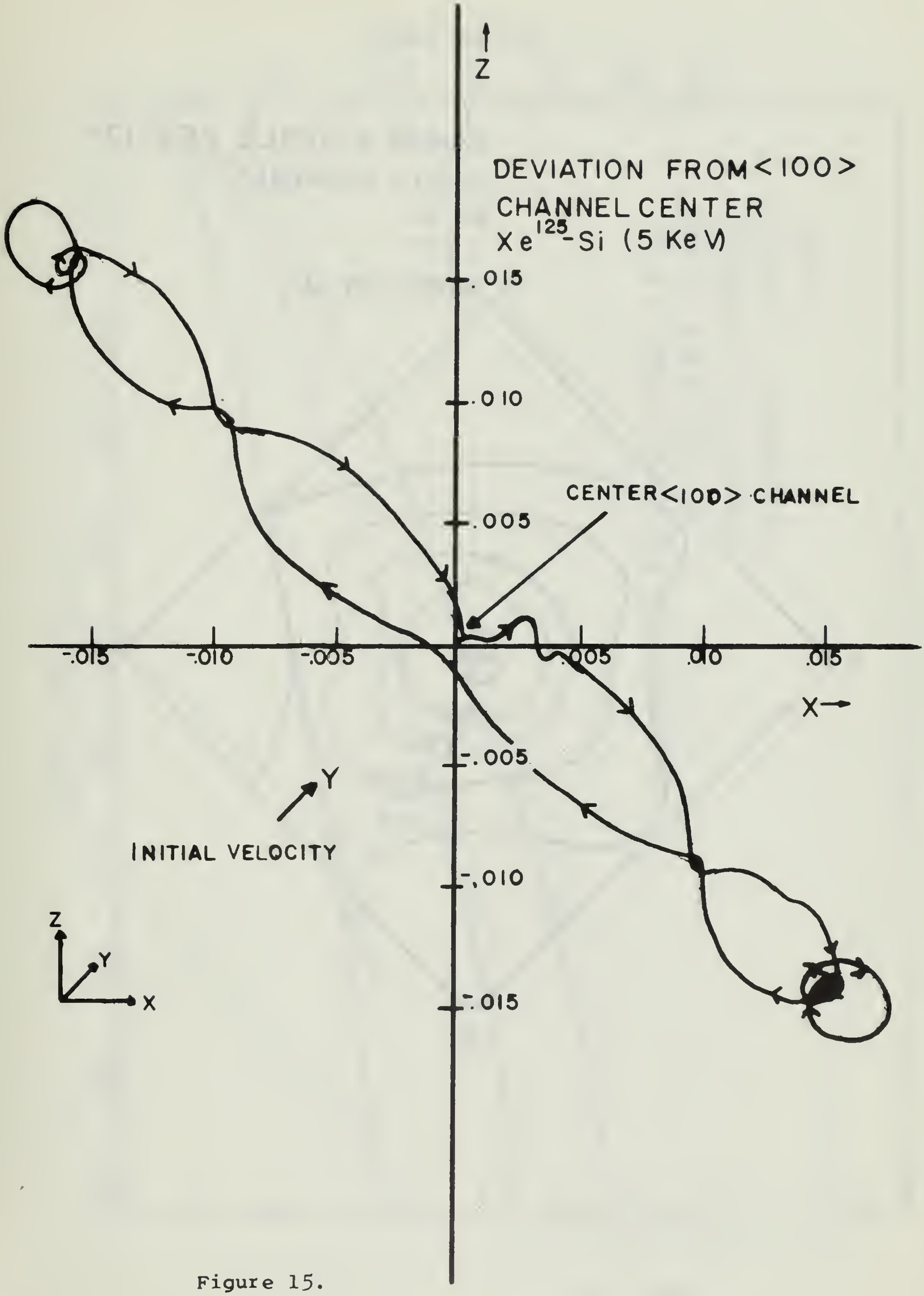
Z
DEVIATION FROM <100>
CHANNEL CENTER
Xe^{125}-Si (5 KeV)
.015
.010
.005
CENTER <100> CHANNEL
-.015
-.010
-.005
.005
.010
.015
X
-.005
-.010
-.015
Y
INITIAL VELOCITY
Z
Y
X

Figure 15.

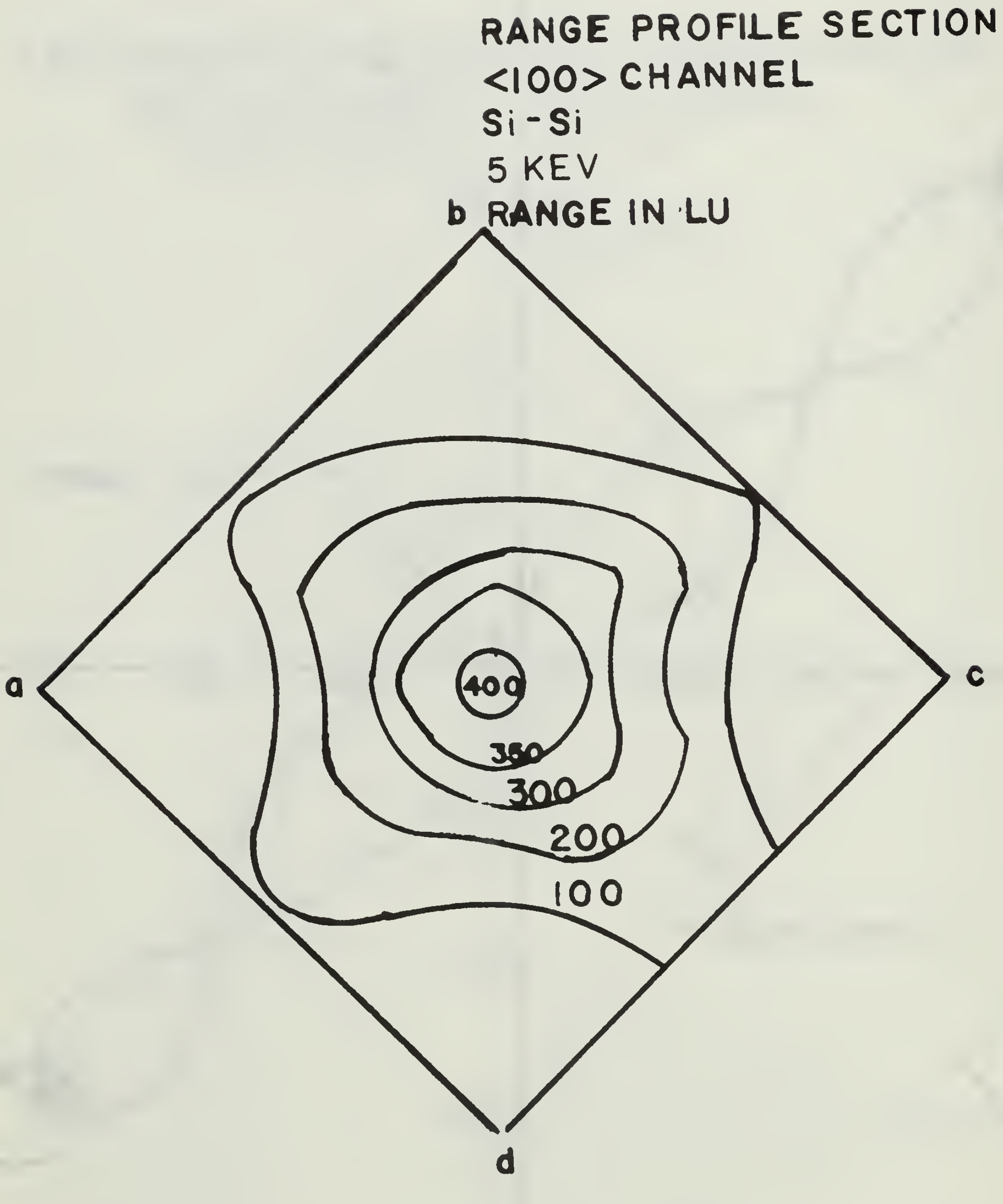

RANGE PROFILE SECTION
<100> CHANNEL
Si - Si
5 KEV
RANGE IN LU
b
a
c
d
400
350
300
200
100

Figure 16.

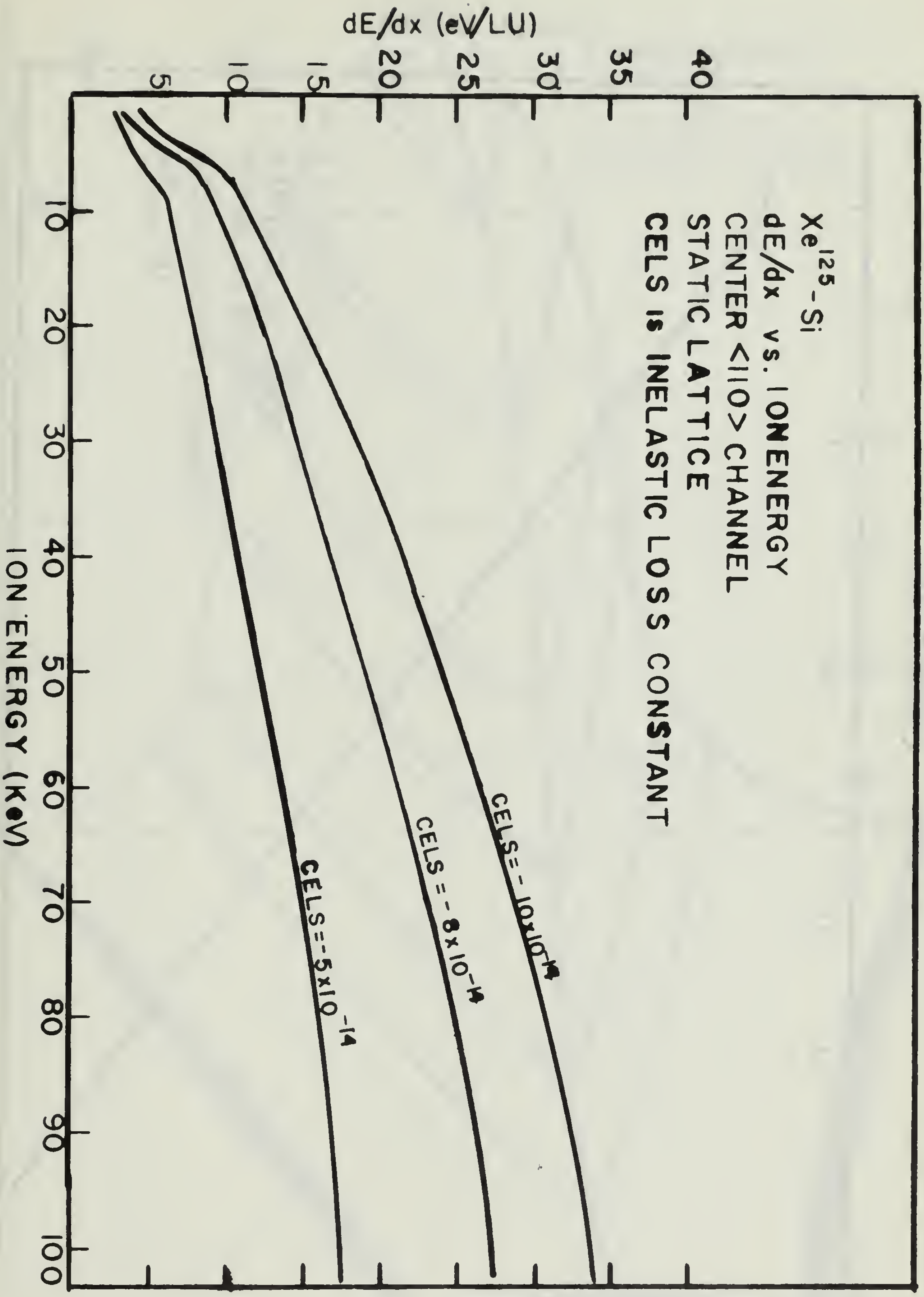
dE/dx (eV/LU)
5
10
15
20
25
30
35
40
10
20
30
40
50
60
70
80
90
100
ION ENERGY (KeV)
Xe125-Si
dE/dx vs. ION ENERGY
CENTER <110> CHANNEL
STATIC LATTICE
CELS is INELASTIC LOSS CONSTANT
CELS=-10x10-14
CELS=-8x10-14
CELS=-5x10-14

Figure 17.

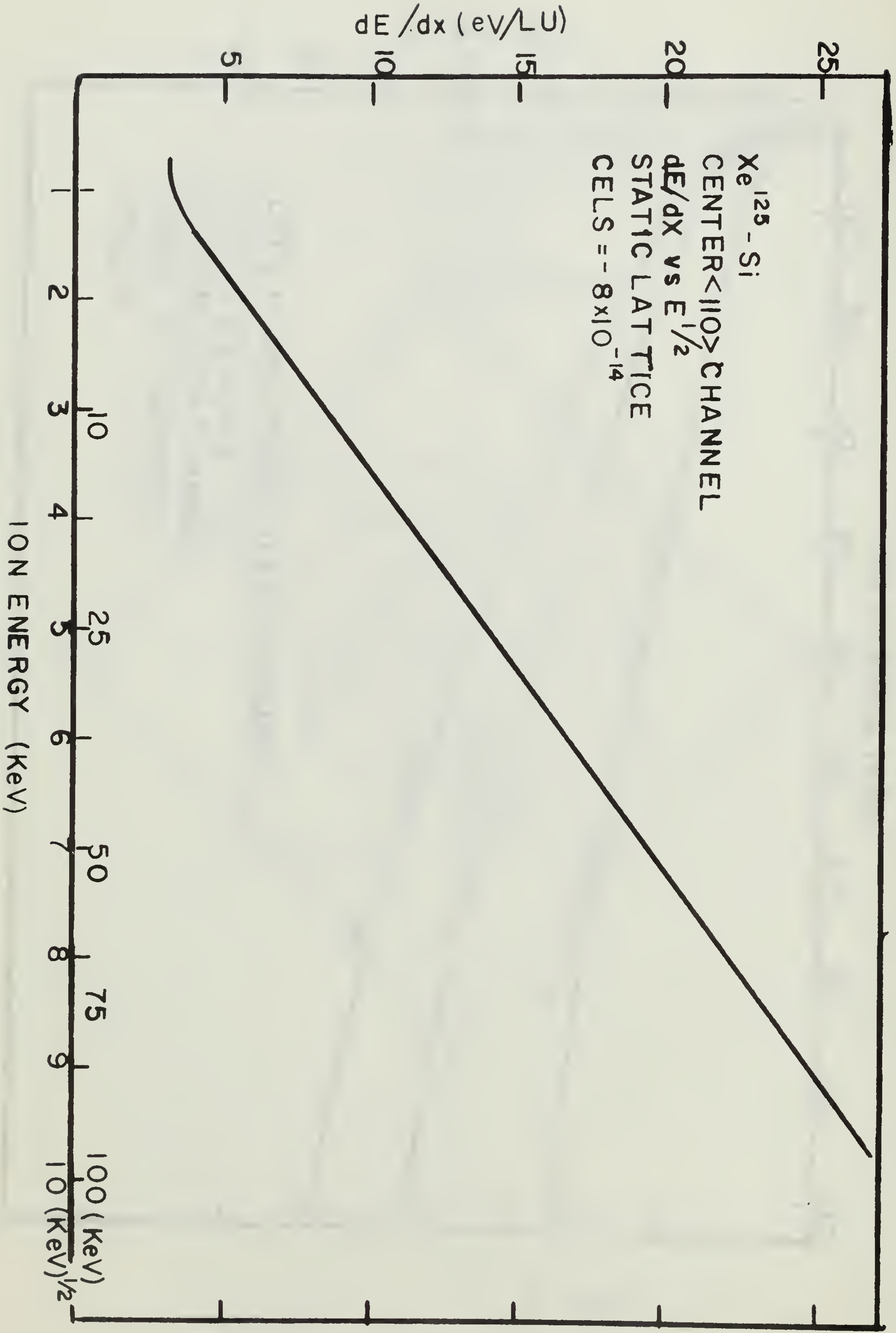
dE/dx (eV/LU)
5
10
15
20
25
Xe125 - Si
CENTER<110> CHANNEL
dE/dX vs E1/2
STATIC LATTICE
CELS = - 8x10-14
1
2
3
4
5
6
7
8
9
10
10
25
50
75
100 (KeV)
(KeV)1/2
ION ENERGY (KeV)

Figure 18.

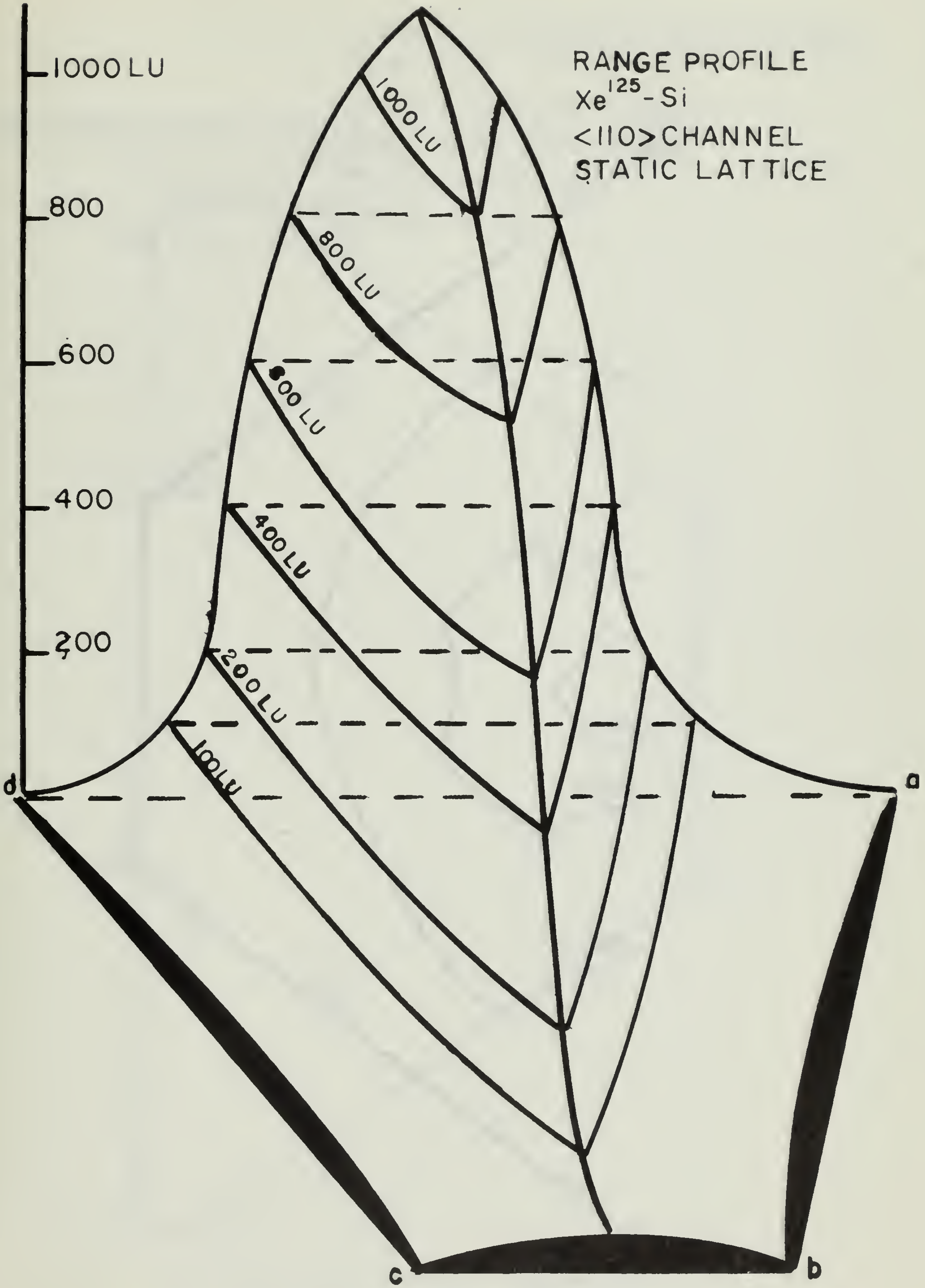
1000 LU
800
600
400
200
RANGE PROFILE
Xe^{125}-Si
<110> CHANNEL
STATIC LATTICE
1000 LU
800 LU
600 LU
400 LU
200 LU
100 LU
d
a
c
b

Figure 19.

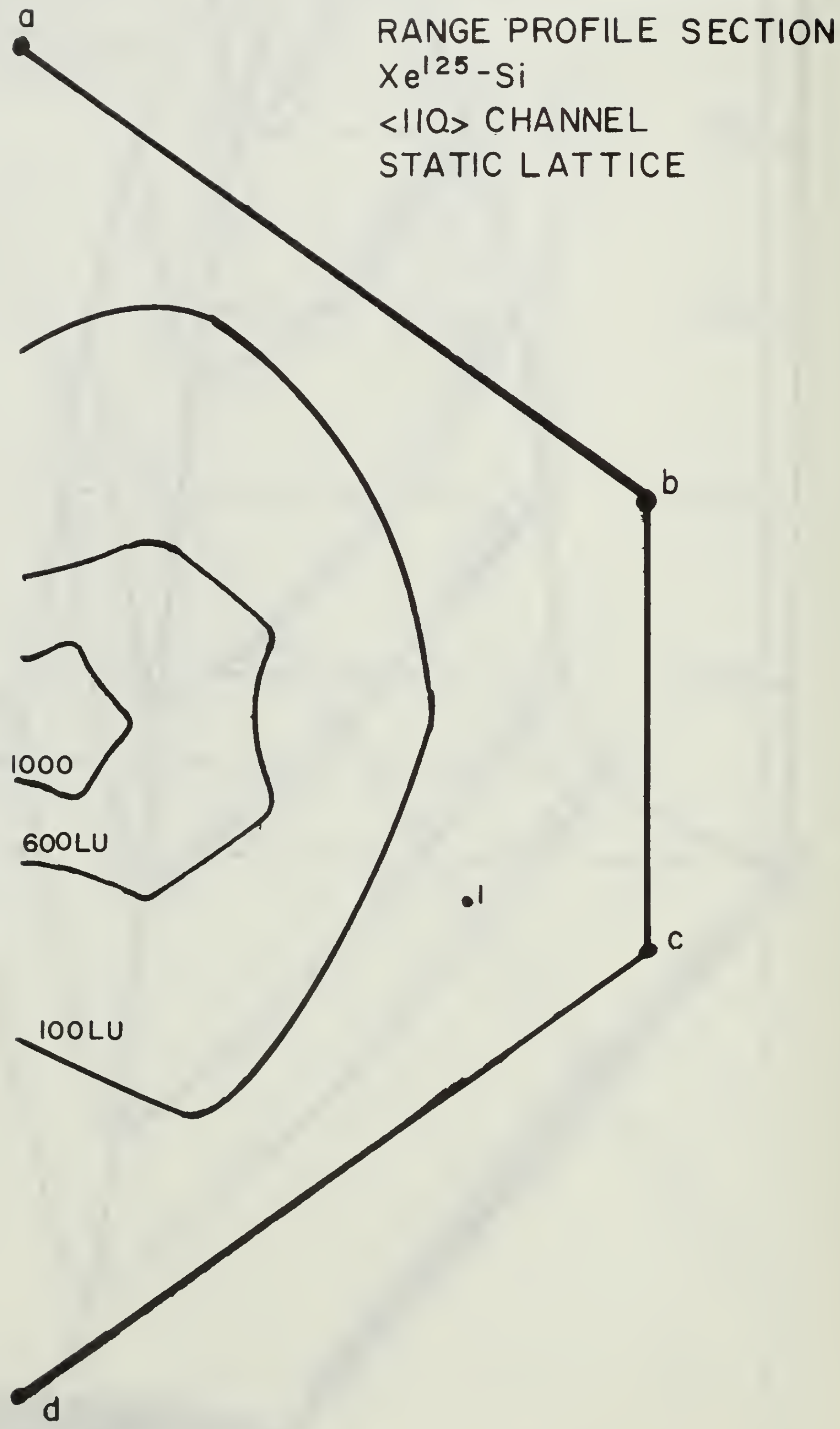
a
RANGE PROFILE SECTION
Xe125-Si
<110> CHANNEL
STATIC LATTICE
b
1000
600LU
1
c
100LU
d

Figure 20.

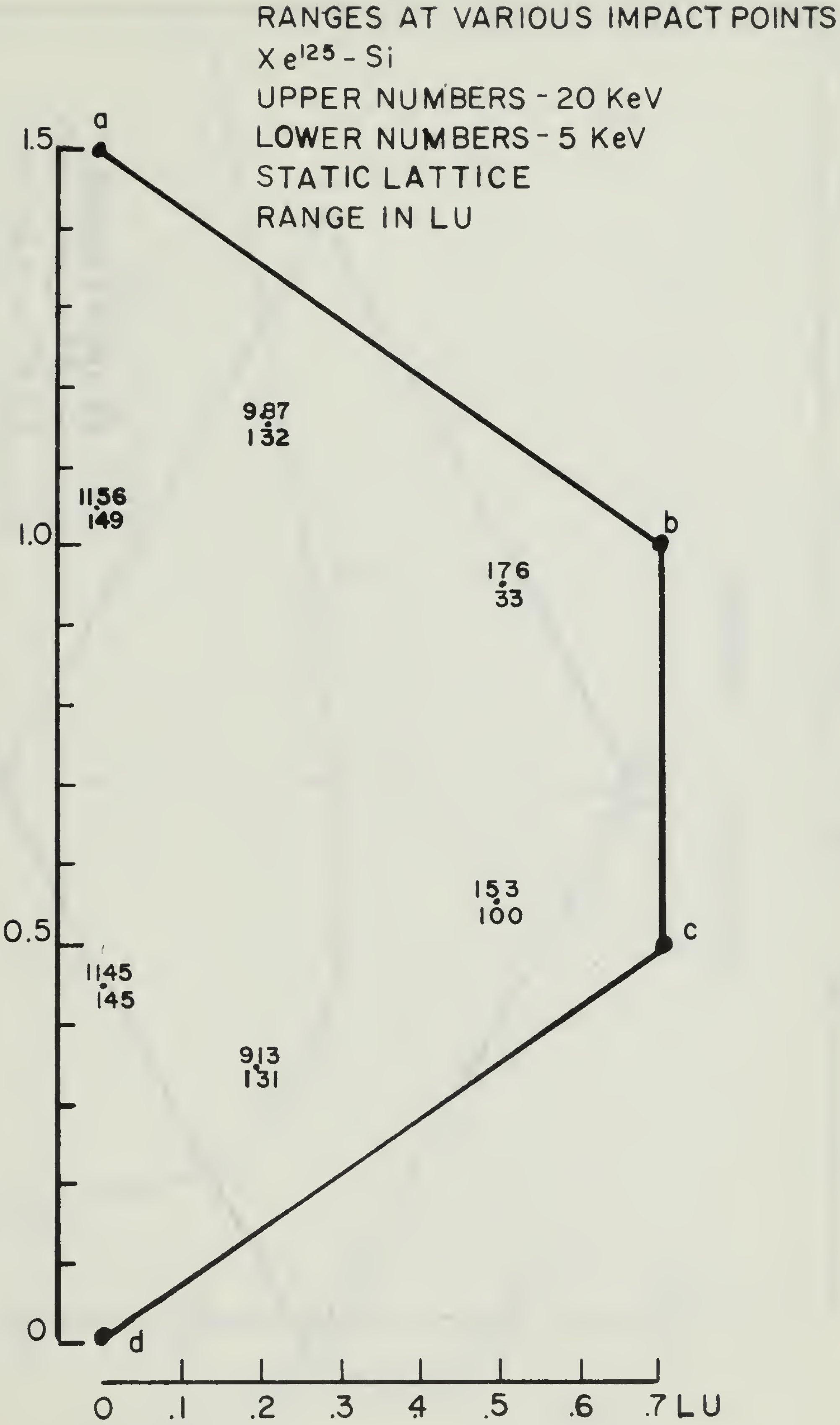
RANGES AT VARIOUS IMPACT POINTS
Xe^{125} - Si
UPPER NUMBERS - 20 KeV
LOWER NUMBERS - 5 KeV
STATIC LATTICE
RANGE IN LU
a
b
c
d
987
132
1156
149
176
33
153
100
1145
145
913
131
1.5
1.0
0.5
0
0
.1
.2
.3
.4
.5
.6
.7 LU

Figure 21.

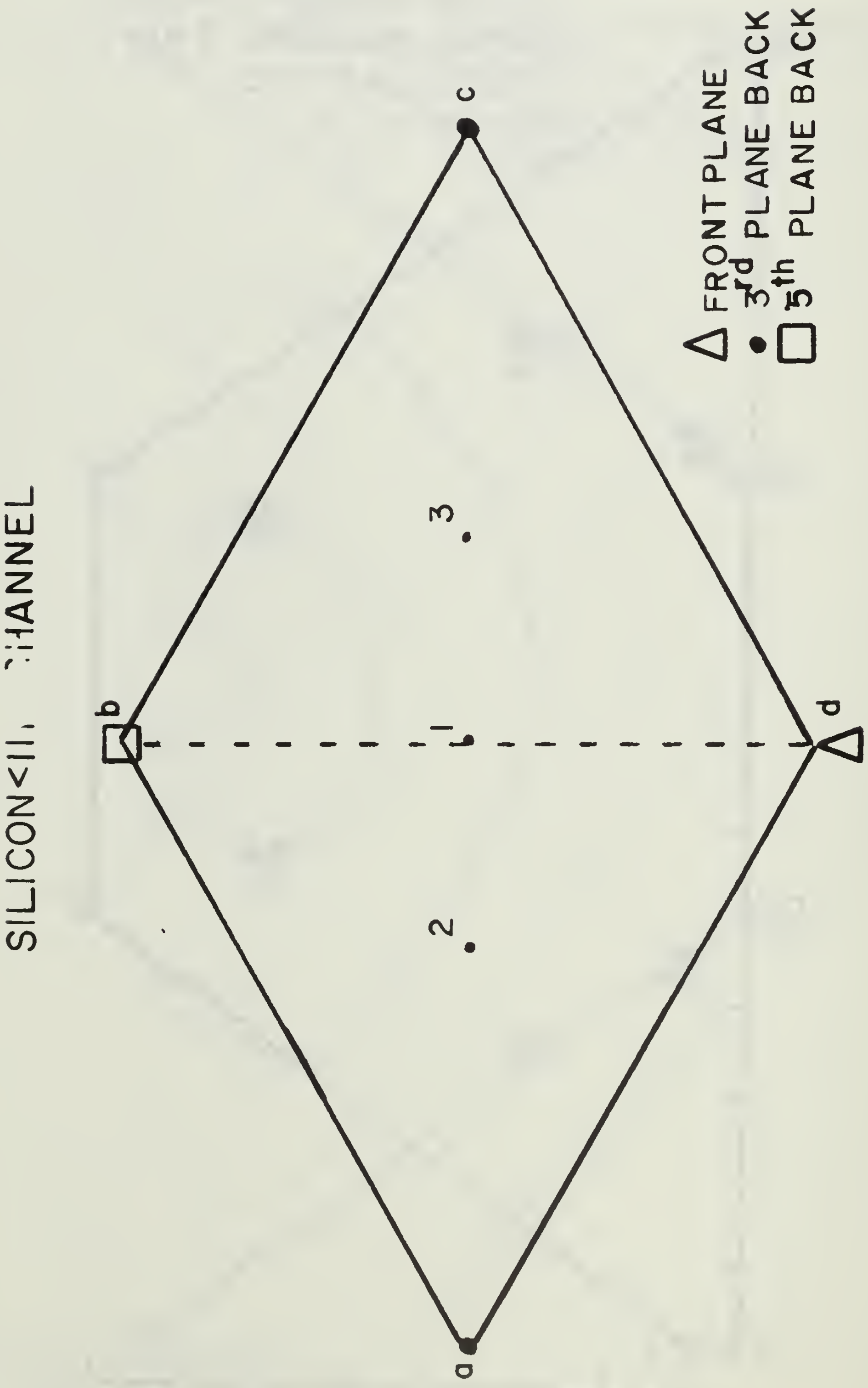
SILICON<111> CHANNEL
a
b
c
d
1
2
3
△ FRONT PLANE
● 3rd PLANE BACK
□ 5th PLANE BACK

Figure 22.

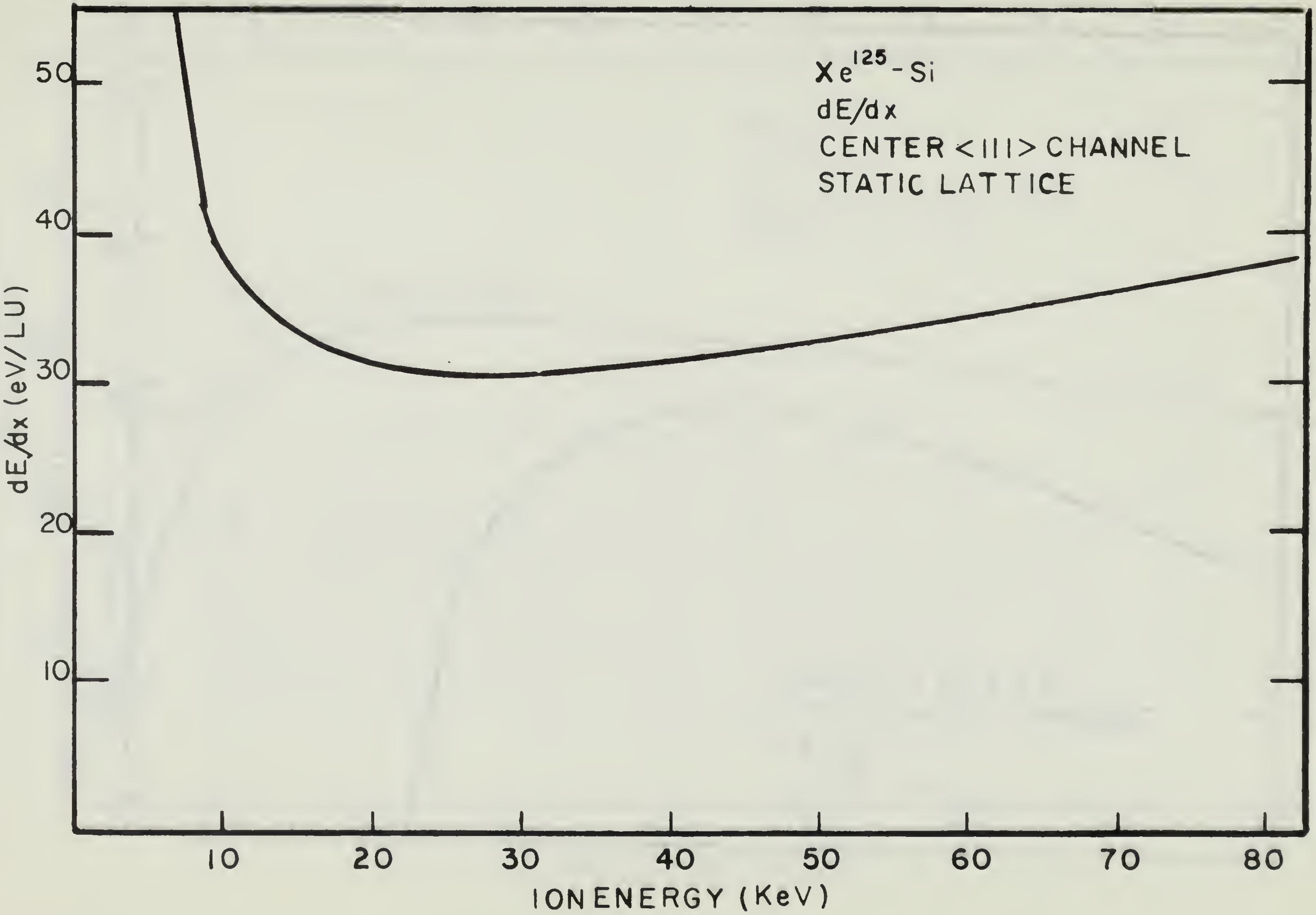
Xe^{125}-Si
dE/dx
CENTER <111> CHANNEL
STATIC LATTICE
dE/dx (eV/LU)
50
40
30
20
10
10
20
30
40
50
60
70
80
IONENERGY (KeV)

Figure 23.

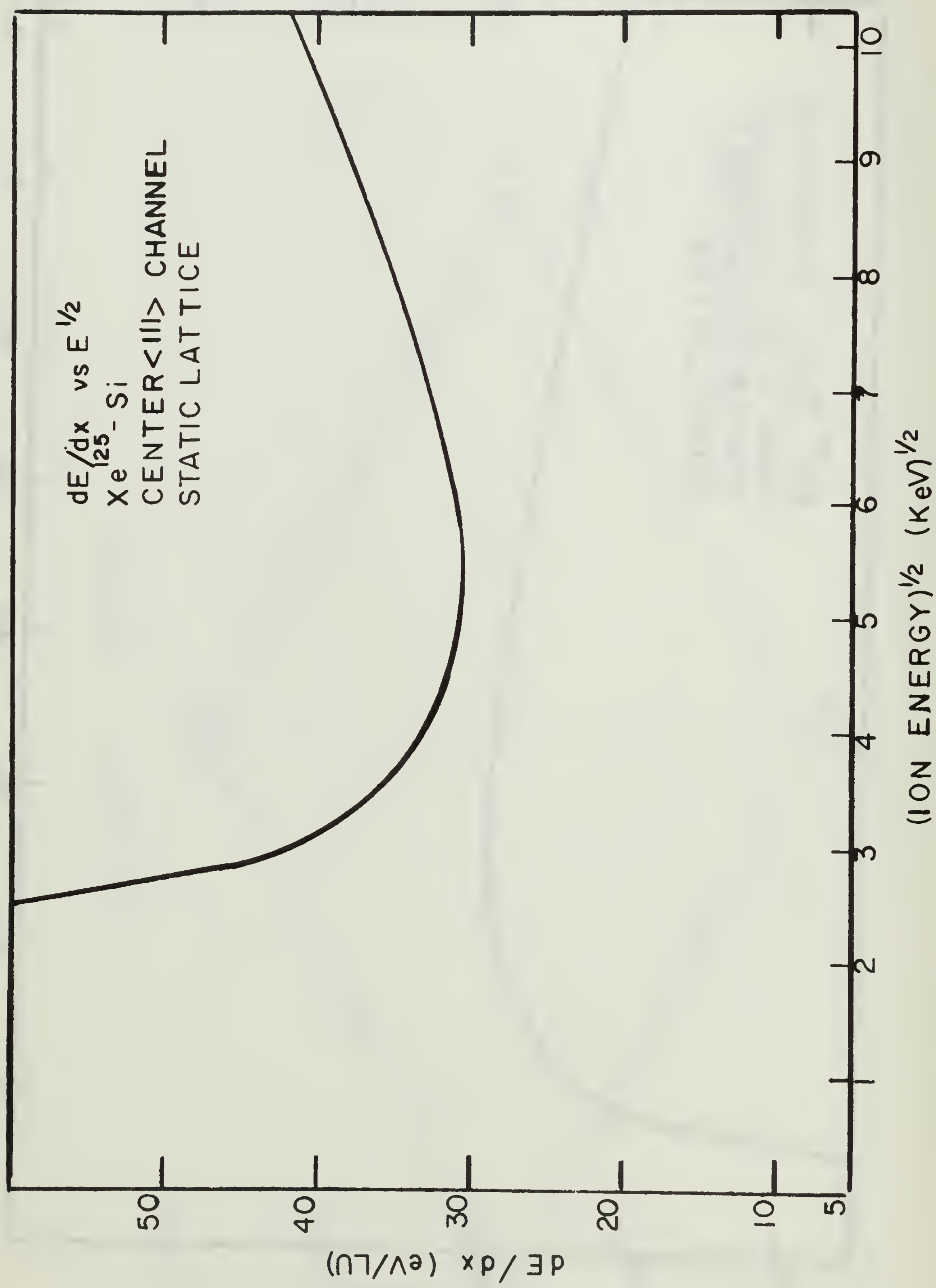
dE/dx vs E 1/2
Xe 125 - Si
CENTER<111> CHANNEL
STATIC LATTICE
50
40
30
20
10
5
dE / dx (eV/LU)
2
3
4
5
6
7
8
9
10
(ION ENERGY)1/2 (KeV)1/2

Figure 24.

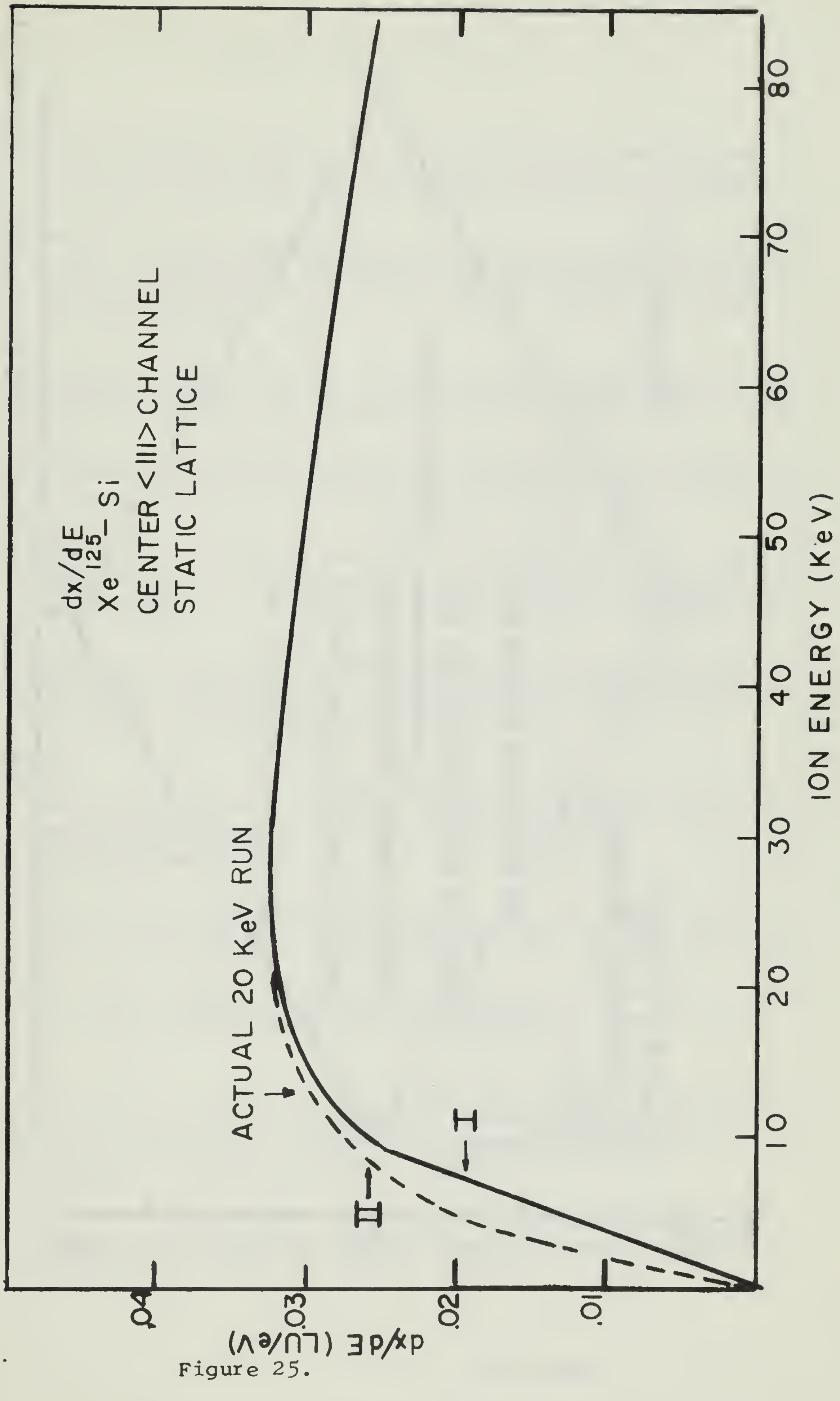
dx/dE
Xe^{125}– Si
CENTER <111> CHANNEL
STATIC LATTICE
ACTUAL 20 KeV RUN
I
II
ION ENERGY (KeV)
10
20
30
40
50
60
70
80
dx/dE (LU/eV)
.01
.02
.03
.04

Figure 25.

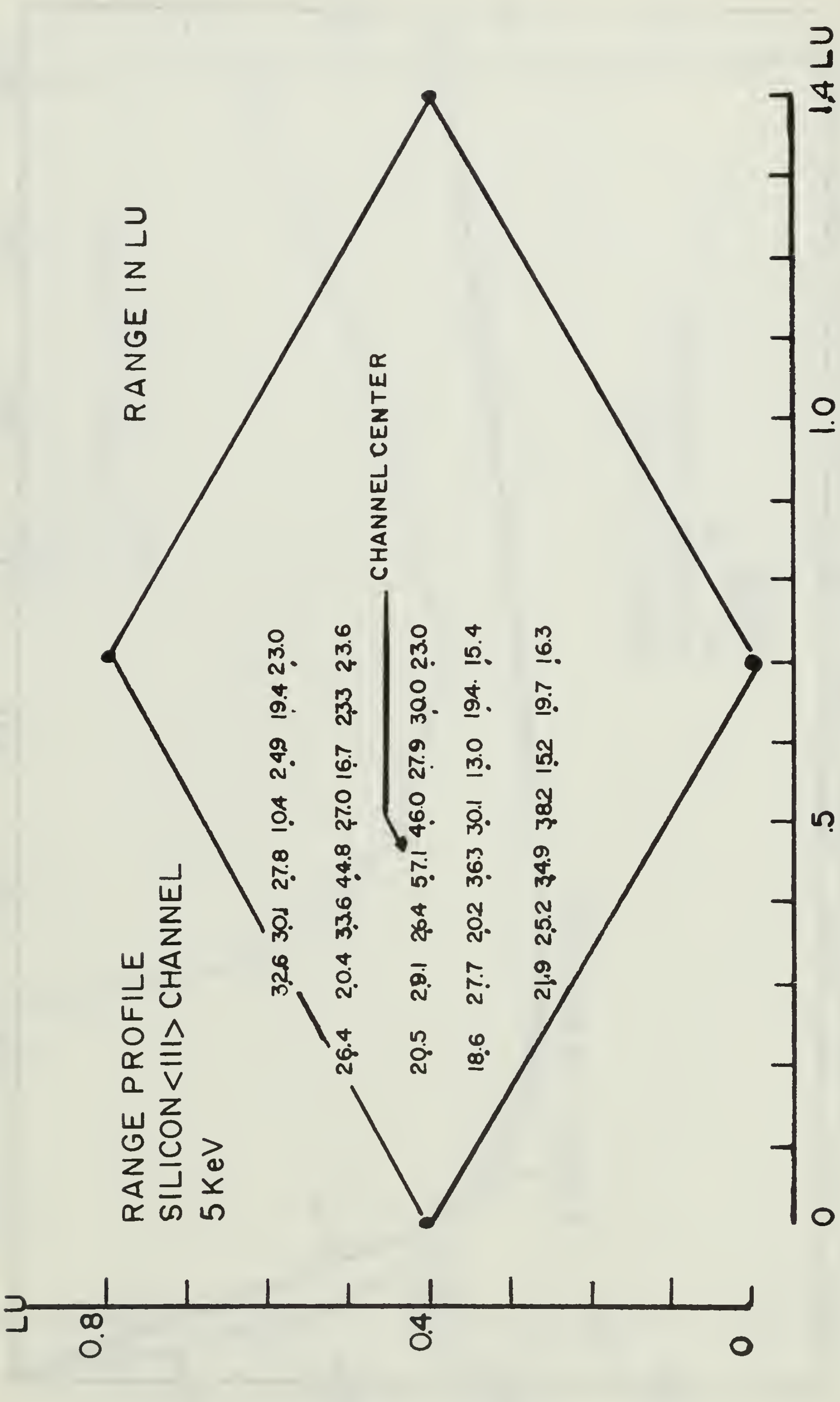
RANGE PROFILE
SILICON <111> CHANNEL
5 KeV
RANGE IN LU
CHANNEL CENTER
32.6 30.1 27.8 10.4 24.9 19.4 23.0
26.4 20.4 33.6 44.8 27.0 16.7 23.3 23.6
20.5 29.1 26.4 57.1 46.0 27.9 30.0 23.0
18.6 27.7 20.2 36.3 30.1 13.0 19.4 15.4
21.9 25.2 34.9 38.2 15.2 19.7 16.3
LU
0.8
0.4
0
0
.5
1.0
1.4 LU

Figure 26.

LIST OF REFERENCES

1. Davies, J.A.,and others, "Range of Energetic Xe^{125} Ions in Monocrystalline Silicon," Canadian Journal of Physics, v. 42, p. 1070-1080, June 1964.

2. Davies, J.A., The Penetration of KeV Projectiles in Solids, paper presented at the HSTM 15th Annual Conference on Mass Spectrometry and Allied Topics, Denver Colorado, USA May 1967.

3. Davies, J.A., and others, "Ion Implantation of Silicon," Canadian Journal of Physics, v. 45, p. 4053-4071, (1967).

4. Davies, J.A., Denhartoy, J., and Whitton, J.L., "Channeling of MeV Projectiles in Tungsten and Silicon," The Physical Review, v. 165 No. 2, p. 345-356, 10 Jan 1968.

5. Gibbons, J.G., "Ion Implantation in Semiconductors - Part I Range Distribution Theory and Experiments," Proceedings of the IEEE, v. 56 No. 3, p. 295-318, March 1968.

6. Harrison, D.E. Jr., and Greiling, D.S., "Computer Studies of Xenon-Ion Ranges in a Finite-Temperature Tungsten Lattice," Journal of Applied Physics, v. 38 No. 8, p. 3200-3211, July 1967.

7. Gay, W.L., and Harrison, D.E., "Machine Simulation of Collisions Between a Copper Atom and a Copper Lattice," The Physical Review, v. 135, p. A1780-A1790, 14 September 1964.

8. Manchester, K.E., "Doping of Silicon by Ion Implantation," Nuclear Instruments and Methods, v. 38, p. 169-174, 1965.

9. Eisen, F.G., "Channeling of Medium Mass Ions Through Silicon," Canadian Journal of Physics, v. 46, p. 561-572, 1968.

10. Mayer, J.W., and others, "Ion Implantation of Silicon and Germanium at Room Temperature, Analysis by Means of 1.0 MeV Helium Ion Scattering," Canadian Journal of Physics, v. 46, p. 663-673, (1968).

11. Glotin, P.M., "Influence of Temperature of Phosphorus Ion Behavior during Silicon Bombardment," Canadian Journal of Physics, v. 46, p. 705-712 (1968).

12. Nelson, R.S., and Mazey, D.J., "The Influence of Temperature and Channeling of Ion-Bombardment Damage in Silicon," Canadian Journal of Physics, v. 46, p. 689-694, (1968).

13. Dearnaley, G., and others, "Implantation Profiles of ^{32}P Channeled into Silicon Crystals," Canadian Journal of Physics, v. 46, p. 587-595 (1968).

14. Eriksson, L., and others, "Implantation and Annealing Behavior of Group III and V Dopants in Silicon as Studied by Channeling Technique," Journal of Applied Physics, v. 40 (2), p. 842-854, Feb 1969.

15. Harrison, D.E., Jr., Leeds, R.W., and Gay, W.L., "Computer Studies of Copper Atom Ranges in Copper Lattices," Journal of Applied Physics, v. 36 No. 10, p. 3154-3161, Oct 1965.

16. Harrison, D.E.,Jr., Gay, W.L., and Effrin, H.M., "An Algorithm for the Calculation of the Classical Equations of Motion of an N-Body System," unpublished.

17. Harrison, D.E.,Jr., "Semiclassical Interaction Potential Functions for Atoms and Ions," to be published.

18. Syrken, Y.K., and Dyatkina, M.E., Structure of Molecules and the Chemical Bond (Translated by Partridge M.A. & Jordon, D.O.) 1st ed., v. 1, Interscience Publishers N.Y. (1968).

19. Eisen, F.E., private communication with D.E. Harrison, Jr.

20. Eriksson, L., Davies, J.A., Jespersgaard, P., "Range Measurement in Orientated Tungsten Single Crystals (0.1-1.0 MeV). I. Electronic and Nuclear Stopping Powers," The Physical Review, v. 161, No. 2, p. 219-234, 10 Sept 1967.

21. Manchester, K.E., "Radiotracer Studies of Ion Implanted Profile Build-Up in Silicon Substrates," Journal of the Electrochemical Society, v. 115 No. 6, p. 656-660, June 1968.

22. Alton, D.G., "A Study of Radiation Damage and Substitutional Chemical Impurity Effects in Single-Crystal Germanium Subjected to 40 KeV. B^+, P^+, Al^+, As^+, and Sb^+, Master Thesis, University of Tennessee, August 1967.

23. Brandt, W., "Channel in Crystals," Scientific American, v. 218 No. 3, p. 91-98, March 1968.

INITIAL DISTRIBUTION LIST

		No. Copies
1.	Defense Documentation Center Cameron Station Alexandria, Virginia 22314	20
2.	Library Naval Postgraduate School Monterey, California 93940	2
3.	Professor Don E. Harrison, Jr. Department of Physics Naval Postgraduate School Monterey, California 93940	5
4.	Cpt. Roy S. Finno 2010 Haring Street Brooklyn, New York 11229	2
5.	LCDR Walter L. Moore SMC #1490 Naval Postgraduate School Monterey, California 93940	1
6.	Defense Atomic Support Agency Department of Defense Washington, D.C. 20301	1
7.	Department of the Army Office of Personnel Operations Attn: OPEN Washington, D.C. 20315	1

Unclassified
Security Classification

DOCUMENT CONTROL DATA - R & D

(Security classification of title, body of abstract and indexing annotation must be entered when the overall report is classified)

1. ORIGINATING ACTIVITY *(Corporate author)*
Naval Postgraduate School
Monterey, California 93940

2a. REPORT SECURITY CLASSIFICATION
Unclassified

2b. GROUP

3. REPORT TITLE
A Computer Study of Channeling in Silicon

4. DESCRIPTIVE NOTES *(Type of report and, inclusive dates)*
Master's Thesis; June 1969

5. AUTHOR(S) *(First name, middle initial, last name)*
Roy S. Finno

6. REPORT DATE
June 1969

7a. TOTAL NO. OF PAGES
80

7b. NO. OF REFS
23

8a. CONTRACT OR GRANT NO.

b. PROJECT NO.

c.

d.

9a. ORIGINATOR'S REPORT NUMBER(S)

9b. OTHER REPORT NO(S) *(Any other numbers that may be assigned this report)*

10. DISTRIBUTION STATEMENT
Distribution of this document is unlimited.

11. SUPPLEMENTARY NOTES

12. SPONSORING MILITARY ACTIVITY
Naval Postgraduate School
Monterey, California 93940

13. ABSTRACT

A computer simulation study of channeling in a diamond lattice. The simulation was done for a xenon ion striking the (100), (110) or (111) surface of a silicon target. Potential functions for the Si-Si lattice bond and the Xe-Si interaction are postulated. The electronic stopping cross section for the ⟨110⟩ channel of silicon is estimated.

This work is a continuation in the development of a computer model formulated at the USNPGS which takes into consideration the displacement of the atoms in the target lattice as well as inelastic energy losses by the primary ion. The lattice was not thermalized and only the repulsive portion of the lattice-lattice potential was utilized. Computed ranges are in good agreement with experimental date.

DD FORM 1 NOV 65 **1473** (PAGE 1)
S/N 0101-807-6811

Unclassified
Security Classification

A-31408

14 KEY WORDS	LINK A		LINK B		LINK C	
	ROLE	WT	ROLE	WT	ROLE	WT
Silicon, channeling						
Electronic stopping cross-section xenon in ⟨110⟩ channel of silicon						
Potential functions silicon-silicon						
Potential functions xenon-silicon						

thesF4465
A computer study of channeling in silico
3 2768 002 00174 5
DUDLEY KNOX LIBRARY